Fortschr. Phys. **46** (1998) 4–5, 363–390

Experimental Primer on the Trapped Ion Quantum Computer

D.J. WINELAND, C. MONROE, W.M. ITANO, B.E. KING, D. LEIBFRIED, D.M. MEEKHOF, C. MYATT, and C. WOOD

National Institute of Standards and Technology, Boulder, CO 80303

Abstract

The development of a quantum computer based on a system of trapped atomic ions is described, following the proposal of Cirac and Zoller. Initial results on a two-bit quantum logic gate are presented, and select experimental issues in scaling the system to larger numbers of ions and gates are treated.

PACS numbers: 32.80.Qk, 42.50.Vk, 89.80.+h

I. Introduction

In its simplest form, a quantum computer is a collection of N two-level quantum systems (quantum bits) which can be prepared in an arbitrary entangled quantum state spanning all 2^N basis states [1, 2]. A quantum computer, unlike its classical counterpart, can thus store and simultaneously process superpositions of numbers. Once a measurement is performed on the quantum computer, the superposition collapses to a single number, which in some cases can jointly depend on all of the numbers previously stored. This gives the potential for massive parallelism in particular algorithms [3], most notably an algorithm which factorizes numbers efficiently [2, 4]. Apart from applications to this and other algorithms [5], creating multi-particle entangled states is of great interest in its own right, from the standpoint of quantum measurements [6] and, for example, for improved signal-to-noise ratio in spectroscopy [7, 8].

Unfortunately, there are very few physical systems which are amenable to the task of quantum computation. This is because a quantum computer must (i) interact very weakly with the environment to preserve coherence of the superpositions, and (ii) interact very strongly with other quantum bits to facilitate the construction of quantum logic gates necessary for computing. In addition to these seemingly conflicting requirements, the quantum bits must be able to be controlled and manipulated in a coherent fashion and be read out with high efficiency.

In 1995, CIRAC and ZOLLER showed that a collection of trapped and cooled atomic ions can satisfy these requirements and form an attractive quantum computer architecture [9]. In their proposal, each quantum bit is derived from a pair of internal energy levels of an individual atomic ion. By using laser beams, the quantum bits are coupled to one another

by virtue of the quantized collective motion of the ions in the trap, mediated by the Coulomb interaction. A reduced version of their scheme was implemented in an experiment on a single trapped ion [10].

This paper concentrates on the trapped ion quantum computer architecture, and covers some of the experimental details involved in conducting simple logic operations between small numbers of trapped ions. Following a brief introduction to ion traps and the interaction between internal and motional states of trapped ions in section II, preliminary experiments involving one ion are reviewed in section III, and particular technical problems in the extension of this scheme to $N > 1$ ions are discussed. Section IV considers the problems of addressing individual ions in a string with lasers and the cross-coupling of the $3N$ quantized modes of motion, and section V characterizes some expected sources of decoherence. The topics covered here are by no means exhaustive, but may give an indication of some of the key problems which may lie ahead in the near future. We have attempted a more complete investigation of the problems in Ref. [11]. For more reviews of the trapped ions quantum computer, see Refs. [12, 13]. Other notable physical systems proposed for quantum computation not covered here include cavity-QED [14] and bulk spin nuclear magnetic resonance [15].

II. Background

A. Internal states and detection

Ions can be confined for days in an ultra-high-vacuum environment with minimal perturbations to their internal atomic structure, and collisions with background gas can be neglected. Even though the ions interact strongly through their mutual Coulomb interaction, the fact that the ions are localized necessarily means that the time-averaged value of the electric field they experience is zero; therefore electric field perturbations are small. Magnetic field perturbations to internal structure are important; however, the coherence time for superposition states of two internal levels can be very long by operating at fields where the energy separation between levels is at an extremum with respect to field. For example, a coherence time exceeding 10 minutes between a pair of $^9Be^+$ ground state hyperfine levels has been observed [16]. It is also possible to employ a ground and excited (metastable) electronic state of a trapped ion as a quantum bit [9]. This option seems difficult at the present time, primarily because the energy splitting is typically in the optical region, requiring extremely high laser frequency stability to drive coherent transitions.

Figure 1a shows a reduced energy level diagram of a single $^9Be^+$ ion. Although many other ion species would also be suitable for quantum computation, we will concentrate on $^9Be^+$ here for concreteness and to make a connection to the experiments at NIST [10, 17]. We will primarily be interested in two electronic states, the $^2S_{1/2}(F = 2, m_F = 2)$ and $^2S_{1/2}(F = 1, m_F = 1)$ hyperfine ground states (denoted by $|\downarrow\rangle$, and $|\uparrow\rangle$, respectively), separated in energy by $\hbar\omega_0$. These long-lived "spin" states will form the basis for a quantum bit. Detection of the spin states can be accomplished using the technique of quantum jumps [18]. By tuning a polarized laser beam to the $|\downarrow\rangle \rightarrow {}^2P_{3/2}$ transition near 313 nm (Fig. 1a), many photons are scattered if the atom is in the $|\downarrow\rangle$ spin state (a "cycling" transition), but essentially no photons are scattered if the atom is in the $|\uparrow\rangle$ spin state. If a modest number of these photons are detected, the efficiency of our ability to discriminate between these two states approaches 100%.

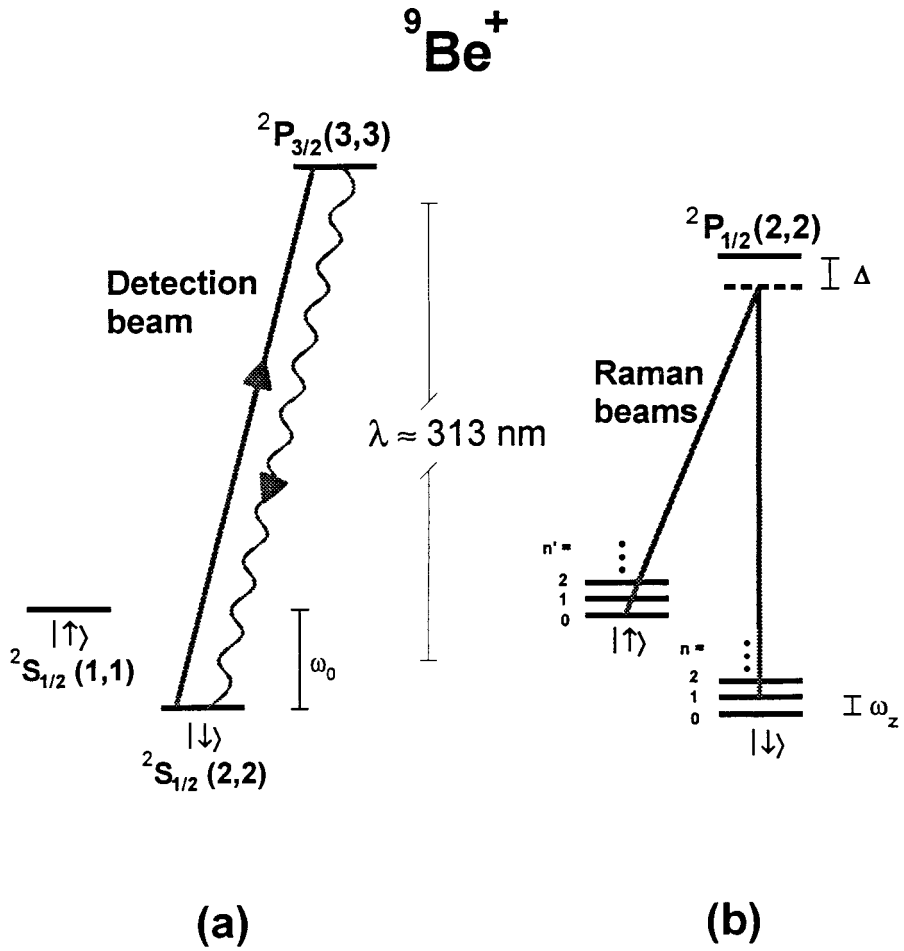

Fig 1: (a) Electronic (internal) energy levels (not to scale) of a $^9Be^+$ ion. The $^2S_{1/2}(F = 2, m_F = 2)$ and $^2S_{1/2}(F = 1, m_F = 1)$ hyperfine ground states (denoted by $|\downarrow\rangle$ and $|\uparrow\rangle$ respectively), separated in frequency by $\omega_0/2\pi \approx 1.250$ GHz, form the basis of a quantum bit. Detection of the internal state is accomplished by illuminating the ion with a σ^+-polarized "detection" beam near 313 nm, which drives the cycling $^2S_{1/2}(F = 2, m_F = 2) \rightarrow {}^2P_{3/2}(F = 3, m_F = 3)$ transition, and observing the scattered fluorescence. The excited P state has radiative linewidth $\gamma/2\pi \approx 19.4$ MHz. (b) Energy levels of a trapped $^9Be^+$ ion, including the motional states of a single mode of harmonic motion, depicted by ladders of vibrational states separated in frequency by the mode frequency ω_z. Two "Raman" beams, both detuned $\Delta \gg \omega_0, \omega_z, \gamma$ (from the excited $^2P_{1/2}$ state, provide a coherent two-photon coupling between states $|n\rangle\,|\downarrow\rangle$ and $|n'\rangle\,|\uparrow\rangle$ by setting the difference frequency ω_L to match the desired transition frequency. As shown, the Raman beams are tuned to the first red sideband of the $|\downarrow\rangle \rightarrow |\uparrow\rangle$ transition ($\omega_L = \omega_0 - \omega_z$).

B. Ion traps and motional states

In Fig. 2, we show a schematic diagram of a linear Paul trap [19], consisting of four electrode rods. The linear trap is similar to a quadrupole mass filter [20] which is plugged at the ends with static electric potentials. A potential $V_0 \cos \Omega_T t$ is applied between diagonally

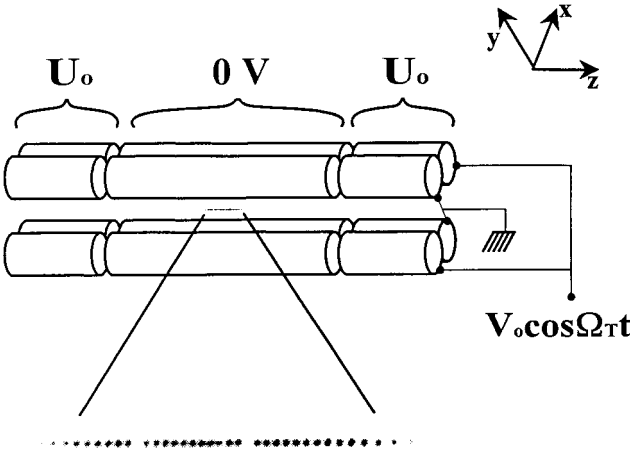

Fig. 2: The upper part of the figure shows a schematic diagram of the electrode configuration for a linear Paul-rf trap (rod spacing $\simeq$1 mm). The lower part of the figure shows an image of a string of $^{199}Hg^{+}$ ions, illuminated with 194 nm radiation, taken with a UV-sensitive, photon counting imaging tube [22]. The spacing between adjacent ions is approximately 10 μm. The "gaps" in the string are occupied by impurity ions, most likely other isotopes of Hg^{+}, which do not fluoresce because the frequencies of their resonant transitions do not coincide with those of the 194 nm $^2S_{1/2} \rightarrow {}^2P_{1/2}$ transition of $^{199}Hg^{+}$.

opposite rods, which are fixed in a quadrupolar configuration, as indicated in Fig. 2. To provide confinement along the axial z direction, static potentials U_0 are applied to the end segments of the rods as indicated. We assume that the rod segments along the z direction are coupled together with capacitors (not shown) so that the rf potential is constant as a function of z. Near the axis of the trap this creates a potential of the form

$$\Phi \simeq \frac{V_0}{2} \cos \Omega_T t \left(1 + \frac{x^2 - y^2}{R^2}\right) + \frac{U_0}{2} \left(\frac{2z^2 - x^2 - y^2}{d^2}\right), \tag{1}$$

where R is equal to the distance from the axis to the surface of the electrode and d is a characteristic axial dimension of the static electrodes. This gives rise to harmonic ponderomotive potentials [21] in the radial (x and y) directions accompanied by static harmonic confinement in the axial (z) direction resulting in an effective $3D$ harmonic confining potential $U(\boldsymbol{r}) = \frac{1}{2} m\omega_x^2 x^2 + \frac{1}{2} m\omega_y^2 y^2 + \frac{1}{2} m\omega_z^2 z^2$, with

$$\omega_x \approx \omega_y \approx \sqrt{\omega_p^2 - \frac{\omega_z^2}{2}}, \qquad \omega_z = \sqrt{\frac{2qU_0}{md^2}}, \tag{2}$$

where $\omega_p \equiv qV_0/(2^{1/2}\Omega_T m R^2)$ describes the ponderomotive portion of the potential, and q and m are the charge and mass of the ion, respectively. In these expressions, it is assumed that $\omega_p \ll \Omega_T$, a condition known as the "pseudopotential approximation" [21].

Figure 2 also shows an image of a "string" of $^{199}Hg^{+}$ ions which are confined near the z axis of the trap described in Ref. [22]. This was achieved by making ω_x, $\omega_y \gg \omega_z$, thereby forcing the ions to the axis of the trap. The spacings between individual ions in this string are governed by a balance of the force along the z direction and the mutual Coulomb repulsion of the ions. Example parameters are given in the figure caption.

Of the $3N$ normal modes of small oscillation in a linear trap, we are primarily interested in the N modes associated with axial motion. A remarkable feature of the linear ion trap is that the axial modes frequencies are nearly independent of N, offering the possibility that mode interference might be small, even for large numbers of ions [9]. For two ions, the axial normal mode frequencies are at ω_z and $\sqrt{3}\omega_z$; for three ions they are

ω_z, $\sqrt{3}\,\omega_z$ and $\sqrt{5.4}\,\omega_z$. For $N > 3$ ions, the Nth axial normal mode can be determined numerically [12, 13, 23]. We will concentrate on the axial center-of-mass (COM) mode, which is the lowest frequency mode and is also the most resolved in frequency from the others. The quantum state of axial COM motion at frequency ω_z can be described by the ladder of vibrational eigenstates $|n\rangle$, of energy $\hbar\omega_z(n+\frac{1}{2})$ with vibrational index n describing the number of "phonons" contained in the collective harmonic COM motion.

C. Coupling between internal and motional states

We describe the coupling between the internal levels of a particular ion in the string with the COM axial mode of collective motion when a classical radiation field is applied to that ion. If the internal levels $|\downarrow\rangle_j$ and $|\uparrow\rangle_j$ of the jth ion in a string are coupled by a dipole moment operator $\boldsymbol{\mu}_j$ (other couplings can be shown to behave analogously), then exposing this ion to a traveling-wave electric field $\boldsymbol{E}(\boldsymbol{r}) = \boldsymbol{E}_0 \cos(\boldsymbol{k}\cdot\boldsymbol{r} - \omega_L t + \varphi)$ with frequency ω_L, phase φ, and wavevector $\boldsymbol{k}$, results in the interaction Hamiltonian

$$\mathscr{H}_I^j = -\boldsymbol{\mu}_j \cdot \boldsymbol{E}(\boldsymbol{r}) = \hbar\Omega^j (S_+^j + S_-^j)\,(e^{i(\boldsymbol{k}\cdot z - \omega_L t + \varphi)} + e^{-i(\boldsymbol{k}\cdot z - \omega_L t + \varphi)})\,. \tag{3}$$

In this expression, $\Omega^j = -\langle\uparrow|\boldsymbol{\mu}_j|\downarrow\rangle \cdot \boldsymbol{E}_0/4\hbar$ is the resonant Rabi frequency connecting $|\downarrow\rangle_j$ to $|\uparrow\rangle_j$ in the absence of confinement, $S_+^j(S_-^j)$ is the internal level raising (lowering) operator of the jth ion changing $|\downarrow\rangle_j$ to $|\uparrow\rangle_j$ and vice-versa, $z = z_0\hat{z}(ae^{-i\omega_z t} + a^\dagger e^{i\omega_z t})$ is the axial COM coordinate operator of the confined motion with associated harmonic raising (lowering) operator $a^\dagger(a)$ and zero-point spread $z_0 \equiv (\hbar/2Nm\omega_z)^{1/2}$, and Nm is the total mass of the ion collection. If the applied radiation frequency is tuned to $\omega_L = \omega_0 + (n'-n)\,\omega_z$, thereby coupling the states $|n\rangle\,|\downarrow\rangle_j$ and $|n'\rangle\,|\uparrow\rangle_j$, $\mathscr{H}_I^j$ is transformed to

$$\mathscr{H}_I^j = \hbar\Omega^j (S_+^j\, e^{i\eta(a+a^\dagger)+i\varphi} + S_-^j\, e^{-i\eta(a+a^\dagger)-i\varphi}) \tag{4}$$

in a frame rotating at ω_L, where terms oscillating faster than Ω^j ($\Omega^j \ll \omega_z, \omega_0$) have been neglected. Here, $\eta \equiv (\boldsymbol{k}\cdot\hat{z})\,z_0$ is the Lamb-Dicke parameter, which controls the amount of coupling between internal and COM motional states.

When the coupling of Eq. (4) is applied between the jth ion and the COM mode of motion, the system evolves between the two quantum states $|n\rangle\,|\downarrow\rangle_j$ and $|n'\rangle\,|\uparrow\rangle_j$ with Rabi frequency [24, 25]

$$\begin{aligned}\Omega_{n',n}^j &\equiv \frac{1}{\hbar}\,|\langle n'|_j\,\langle\uparrow|\,\mathscr{H}_I^j\,|\downarrow\rangle_j\,|n\rangle| \\ &= \Omega^j\,|\langle n'|\,e^{i\eta(a+a^\dagger)}\,|n\rangle| = \Omega^j \eta^{|n'-n|}\,e^{-\eta^2/2}\,\sqrt{\frac{n_<!}{n_>!}}\,L_{n_<}^{|n'-n|}(\eta^2)\,,\end{aligned} \tag{5}$$

where $n_>(n_<)$ is the greater (lesser) of n and n' and $L_n^\alpha(x)$ is a generalized Laguerre polynomial. If the Lamb-Dicke criterion is satisfied, where the amplitude of the ion's motion in the direction of the radiation is much less than $\lambda/2\pi$ (or $n^{1/2}\eta \ll 1$), we can evaluate $\Omega_{n',n}^j$ to lowest order in η to obtain

$$\Omega_{n',n}^j = \Omega^j\,\frac{\eta^{|n'-n|}}{|n'-n|!}\,\sqrt{\frac{n_>!}{n_<!}}\,. \tag{6}$$

We will be primarily interested in three types of transitions – the carrier ($n' = n$), the first red sideband ($n' = n - 1$), and the first blue sideband ($n' = n + 1$) whose Rabi frequencies, in the Lamb-Dicke limit, are given from Eq. (6) by Ω^j, $\eta n^{1/2}\Omega^j$, and $\eta(n+1)^{1/2}\Omega^j$ respectively.

In practice, driving direct transitions between $|n\rangle|\downarrow\rangle_j$ and $|n'\rangle|\uparrow\rangle_j$ with rf or microwave radiation is not be feasible, as the sideband operation transition rates (proportional to $\eta = 2\pi z_0/\lambda$) would be extremely slow due to the long wavelength of the radiation. Alternatively, optical fields can be used to drive two-photon stimulated Raman transitions between $|n\rangle|\downarrow\rangle_j$ and $|n'\rangle|\uparrow\rangle_j$ [17, 26]. As depicted in Fig. 1b, two laser beams detuned by Δ from an excited state of radiative width γ are applied to the jth ion with their difference frequency matched to the desired transition frequency. For sufficient detuning $|\Delta| \gg \gamma$, the excited state may be adiabatically eliminated, and the above couplings apply, with Ω^j replaced by $g_1^j g_2^j/\Delta$, where g_1^j and g_2^j are the individual Rabi frequencies of the two beams when resonantly coupled to the excited level. In addition, $\omega_L(\varphi)$ is replaced by the difference frequency (phase) of the beams; and $\boldsymbol{k}$ is replaced by the difference in wavevectors of the two Raman beams $\delta\boldsymbol{k} = \boldsymbol{k}_1 - \boldsymbol{k}_2$. Since the relevant frequency depends only on the microwave difference between the two laser frequencies, both beams can be generated with a single laser source and a modulator, thereby relaxing the constraints of laser frequency stabilization. The use of stimulated Raman transitions thus combines the advantages of the strong couplings with the frequency stability of microwave sources [26, 27].

D. Laser cooling to the motional ground state

As a starting point for trapped ion quantum computing, the ions must be initialized in known pure states. Using standard optical pumping techniques, we can prepare the ions in the $|\downarrow\rangle$, internal state. Laser cooling in the resolved sideband limit [25] can, for single ions, generate the $|n = 0\rangle$ motional state with reasonable efficiency [17, 28]. This type of laser cooling is usually preceded by a stage of "Doppler" laser cooling [29] which typically cools the ion to $\langle n\rangle \geq 1$, or an equivalent temperature of about 1 mK.

Resolved sideband laser cooling for a single, harmonically-bound atom can be explained as follows: For simplicity, we assume the atom is confined by a 1-D harmonic well of vibration frequency ω_z. We use an optical transition whose radiative linewidth γ is relatively narrow, $\gamma \ll \omega_z$ (Doppler laser cooling applies when $\gamma \geq \omega_z$). If a laser beam (frequency ω_L) is incident along the direction of the atomic motion, the bound atom's absorption spectrum is composed of a "carrier" at frequency ω_0 and resolved frequency-modulation sidebands that are spaced by ω_z. These sidebands in the spectrum are generated from the Doppler effect (like vibrational substructure in a molecular optical spectrum). Laser cooling can occur if the laser is tuned to a lower (red) sideband, for example, at $\omega_L = \omega_0 - \omega_z$. In this case, photons of energy $\hbar(\omega_0 - \omega_z)$ are absorbed, and spontaneously emitted photons of average energy $\hbar\omega_0 - R$ return the atom to its initial internal state, where $R \equiv (\hbar k)^2/2m = \hbar\omega_R$ is the photon recoil energy of the atom. Overall, for each scattering event, this reduces the atom's kinetic energy by $\hbar\omega_z$ if $\omega_z \gg \omega_R$, a condition which is satisfied for ions in strong ion traps. Since $\omega_R/\omega_z = \eta^2$ where η is the Lamb-Dicke parameter, this simple form of sideband cooling requires that the Lamb-Dicke parameter be small. For example, in $^9Be^+$, if the recoil corresponds to spontaneous emission from the 313 nm $^2P_{1/2} \rightarrow {}^2S_{1/2}$ transition (typically used for laser cooling), $\omega_R/2\pi \simeq 230$ kHz. This is to be compared to trap oscillation frequencies in some laser-cooling experiments of around 10 MHz [17]. Cooling proceeds until the atom's mean vibrational quantum number in the harmonic well is given by $\langle n\rangle_{\min} \simeq (\gamma/2\omega_z)^2 \ll 1$ [29]. As discussed above, it is convenient to use two-photon stimulated Raman transitions for sideband cooling [17, 30], but the basic idea for, and limits to, cooling are essentially the same as for single-photon transitions.

Although laser cooling to the $|n = 0\rangle$ state has been achieved with single ions [17, 28]; a prerequisite to future work is to laser cool a collection of ions (or, at least one mode of the collection) to the zero-point state. Cooling of any of the $3N$ modes of motion of a collection of ions should, in principle, work the same as cooling of a single ion. To cool a particular mode, we tune the cooling radiation to its first lower sideband. If we want to cool all modes, sideband cooling must be cycled through all $3N$ modes more than once, or applied to all $3N$ modes at once, since recoil will heat all modes. For the COM mode, the cooling is essentially the same as cooling a single particle of mass Nm; however, the recoil energy upon re-emission is distributed over all $3N$ modes. Other methods to prepare atoms in the $|n = 0\rangle$ state are discussed in Refs. [31]. In Ref. [32], it is shown that it is not necessary to satisfy the condition $\omega_R \ll \omega_z$ $(\eta \ll 1)$ to achieve cooling to $n = 0$.

III. Quantum Logic with Trapped Ions

Several authors have shown that an arbitrary unitary operation (therefore any quantum computation) on a collection of quantum bits can be broken into a series of fundamental single bit and dual bit quantum logic gates [33]. This is similar to classical computing, where certain families of logic gates are universal (for instance, the single bit NOT and two bit AND gates). One such family of universal quantum logic gates consists of the single bit rotation gate and the two-bit controlled-NOT gate [34]. For brevity, we concentrate on these two gates and how they can be implemented in a system of trapped ions.

The single bit rotation gate [operator $R(\theta, \varphi)$] simply changes the state of a single quantum bit and is characterized by the following transformation:

$$\begin{aligned} |\downarrow\rangle &\rightarrow \cos(\theta/2)\,|\downarrow\rangle - i\,e^{i\varphi}\sin(\theta/2)\,|\uparrow\rangle \\ |\uparrow\rangle &\rightarrow \cos(\theta/2)\,|\uparrow\rangle - i\,e^{-i\varphi}\sin(\theta/2)\,|\downarrow\rangle\,, \end{aligned} \tag{7}$$

where θ and φ are parameters of the gate. This transformation is commonplace in atomic physics and nuclear magnetic resonance, and has been widely applied to two level systems. In the context of trapped ions, the single bit rotation gate is accomplished by tuning to the carrier transition $(\omega_L = \omega_0)$ and applying radiation for a time t such that $\theta = 2\Omega^j t$ (Eq. (6)). The parameter θ describes the "rotation" between the two spin states ($\theta = \pi$ is called a "π" pulse, etc.), and the parameter φ describes the phase of the rotation. Figure 3 depicts the observed Rabi flopping between $|\downarrow\rangle$, and $|\uparrow\rangle$, states in a single trapped $^9Be^+$ ion

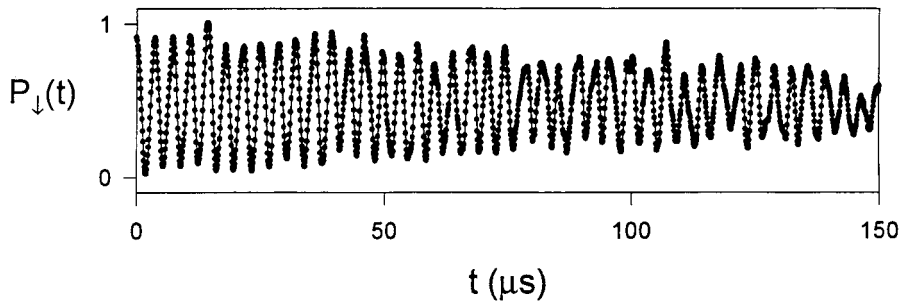

Fig. 3: Experimental plot of the probability $P_\downarrow(t)$ of finding a single $^9Be^+$ ion in the $|\downarrow\rangle$ state after first preparing it in the $|\downarrow\rangle$ state and applying the carrier coupling (Eq. (7)) for a time t, with $\theta/2 = \Omega^j t$. $P_\downarrow(t)$ does not follow a perfect sinusoid due to decoherence, described in section IV. Each point represents an average of 4000 observations.

according to the above transformation [35]. The ion is first prepared in the $|\downarrow\rangle$, state, then the carrier transition is applied for a time t, and the state ($|\downarrow\rangle$, or $|\uparrow\rangle$) is detected as described above and in Fig. 1a.

A more nontrivial quantum logic gate is the two-bit controlled-NOT (CN) gate [33, 34], reminiscent of the classical XOR gate. This gate flips the spin of ion k, the "target bit" ($|\downarrow\rangle_k \leftrightarrow |\uparrow\rangle_k$) if and only if ion j, the "control bit," is in state $|\uparrow\rangle$. The transformation of the two quantum bits j and k are as follows:

$$\begin{aligned} |\downarrow\rangle_j |\downarrow\rangle_k &\rightarrow |\downarrow\rangle_j |\downarrow\rangle_k \\ |\downarrow\rangle_j |\uparrow\rangle_k &\rightarrow |\downarrow\rangle_j |\uparrow\rangle_k \\ |\uparrow\rangle_j |\downarrow\rangle_k &\rightarrow |\uparrow\rangle_j |\uparrow\rangle_k \\ |\uparrow\rangle_j |\uparrow\rangle_k &\rightarrow |\uparrow\rangle_j |\downarrow\rangle_k . \end{aligned} \tag{8}$$

CIRAC and ZOLLER [9] showed how the above transformation could be accomplished between two of a collection of trapped ions by utilizing a motional mode (i.e., axial COM mode) as a "data bus" through which the quantum bits are shuttled. As described above, the COM mode is assumed to be initially cooled to the $|n = 0\rangle$ ground state. The scheme is outlined as follows:

(1) Map the state of ion j (spanning the states $|\downarrow\rangle_j$, $|\uparrow\rangle_j$) onto the first two axial COM motional states (spanning the states $|n = 0\rangle$, $|n = 1\rangle$) shared amongst all ions.
(2) Flip the spin state of ion k ($|\downarrow\rangle_k \leftrightarrow |\uparrow\rangle_k$) if and only if there is a phonon in the COM mode.
(3) Reverse step (1): map the state of the motion back onto ion j.

The central ingredient here is step (2), which is itself a "reduced" CN gate, with the first two motional states acting as the control bit and ion k acting as the target bit

$$\begin{aligned} |0\rangle |\downarrow\rangle_k &\rightarrow |0\rangle |\downarrow\rangle_k \\ |0\rangle |\uparrow\rangle_k &\rightarrow |0\rangle |\uparrow\rangle_k \\ |1\rangle |\downarrow\rangle_k &\rightarrow |1\rangle |\uparrow\rangle_k \\ |1\rangle |\uparrow\rangle_k &\rightarrow |1\rangle |\downarrow\rangle_k . \end{aligned} \tag{9}$$

This last transformation has been realized on a single trapped ion [10]. In that experiment, performed on a trapped $^9Be^+$ ion, the control bit was one of the three modes of the ion's motion. The reduced CN operation between these states (step (2) above) was realized by applying three laser pulses in succession:

(a) A $\pi/2$ pulse ($\Omega^k t = \pi/4$ in Eq. (6)) is applied on the carrier transition. For a certain choice of initial phase, this corresponds to the rotation operator $R(\theta = \pi/2, \varphi)$.
(b) A 2π pulse is applied on the first blue sideband transition between levels $|\uparrow\rangle$ and an auxiliary level $|\text{aux}\rangle$ in the ion (the $|F = 2, M_F = 0\rangle$ level in $^9Be^+$; see Fig. 4). This operation provides the "conditional dynamics" for the overall CN operation. It changes the sign of the $|1\rangle |\uparrow\rangle$ component of the wavefunction but leaves the sign of the $|0\rangle |\uparrow\rangle$ component of the wavefunction unchanged; that is, the sign change is conditioned on whether or not the ion is in the $|0\rangle$ or $|1\rangle$ motional state.
(c) A $\pi/2$ pulse is applied to the spin carrier transition with a 180° phase shift relative to step (a). This corresponds to the operator $R(\theta = \pi/2, \varphi + \pi)$.

Steps (a) and (c) can be regarded as two resonant pulses of opposite phase in the RAMSEY separated-field method of spectroscopy [36]. If step (b) is active (thereby changing the sign

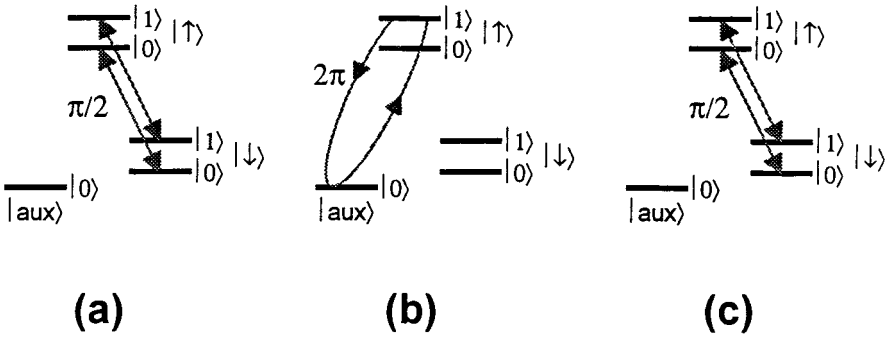

Fig. 4: Energy levels of a single trapped $^9Be^+$ ion, including the internal hyperfine levels $|\downarrow\rangle$ and $|\uparrow\rangle$ and an auxiliary level $|\text{aux}\rangle$ [the $^2S_{1/2}(F=2, m_F=0)$ state], each dressed by the lowest two motional quantum harmonic oscillator states $|n\rangle = |0\rangle$ and $|1\rangle$. The controlled-NOT quantum logic gate results in a spin flip ($|\downarrow\rangle \leftrightarrows |\uparrow\rangle$ if and only if $|n\rangle = |1\rangle$. This transformation is realized with a sequence of three pulses of laser light which couple the states indicated by the arrows: **(a)** A $\pi/2$ pulse couples states $|n\rangle|\downarrow\rangle$ to $|n\rangle|\uparrow\rangle$. **(b)** A 2π pulse couples state $|1\rangle|\uparrow\rangle$ to $|0\rangle|\text{aux}\rangle$, resulting in a sign change of any component in the $|1\rangle|\uparrow\rangle$ state. **(c)** A $-\pi/2$ pulse couples states $|n\rangle|\downarrow\rangle$ to $|n\rangle|\uparrow\rangle$ (same as step (a) with a π phase shift). If $|n\rangle = |0\rangle$, then step (b) is inactive since it only affects to the $|1\rangle|\uparrow\rangle$ state, and the two $\pi/2$ pulses cancel, leaving the initial state unaffected. If $|n\rangle = |1\rangle$, then the sign change in step (b) causes the two $\pi/2$ pulses to add, resulting in a net spin flip ($|\downarrow\rangle \leftrightarrows |\uparrow\rangle$). The result is the transformation of Eq. (9).

of the $|1\rangle|\uparrow\rangle$ component of the wavefunction), then a spin flip is induced by the Ramsey fields. If step (b) is inactive, step (c) reverses the effect of step (a).

Instead of the three pulses (a–c above), a simpler CN gate scheme between an ion's internal and motional states can be achieved with a single laser pulse, while eliminating the requirement of the auxiliary internal electronic level [37]. By applying a single pulse tuned to the carrier transition, from Eq. (5), the states $|n\rangle|\downarrow\rangle$ and $|n\rangle|\uparrow\rangle$ are coupled with Rabi frequency

$$\Omega_{n,n} = \Omega\,|\langle n|\, e^{i\eta(a+a^\dagger)}\,|n\rangle| = \Omega\, e^{-\eta^2/2}\,\mathscr{L}_n(\eta^2)\,, \tag{10}$$

where $\mathscr{L}_n(\eta^2) \equiv L_n^0(\eta^2)$ is a Laguerre polynomial. Specializing to the $|n\rangle = |0\rangle$ and $|n\rangle = |1\rangle$ vibrational levels relevant to quantum logic, we have

$$\begin{aligned} \Omega_{0,0} &= \Omega\, e^{-\eta^2/2}\,, \\ \Omega_{1,1} &= \Omega\, e^{-\eta^2/2}(1-\eta^2)\,. \end{aligned} \tag{11}$$

The CN gate can be achieved in a single pulse by setting η so that $\Omega_{1,1}/\Omega_{0,0} = (2k+1)/2m$, with k and m positive integers satisfying $m > k \geq 0$. Setting $\Omega_{1,1}/\Omega_{0,0} = 2m/(2k+1)$ will also work, with the roles of the $|0\rangle$ and $|1\rangle$ motional states switched in Eq. (10). By driving the carrier transition for a duration τ such that $\Omega_{1,1}\tau = (k+\frac{1}{2})\,\pi$, or a "$\pi$-pulse" (mod 2π) on the $|n\rangle = |1\rangle$ component, this forces $\Omega_{0,0}\tau = m\pi$. Thus the states $|\downarrow\rangle|1\rangle \leftrightarrow |\uparrow\rangle|1\rangle$ are swapped, while the states $|\downarrow\rangle|0\rangle$ and $|\uparrow\rangle|0\rangle$ remain unaffected. This transformation is equivalent to the reduced CN of Eq. (9), apart from phase factors which can be eliminated by the appropriate settings of the phase of subsequent logic operations.

The mapping steps (steps (1) and (3) above) can be realized by applying a π-pulse on the red sideband of ion j. This accomplishes the mapping $|0\rangle(\alpha|\downarrow\rangle_j + \beta|\uparrow\rangle_j) \rightarrow (\alpha|0\rangle$

$+\beta\,|1\rangle)\,|\downarrow\rangle_j$. Analogous mapping of internal state superpositions to motional state superpositions of a trapped ion has also been reported in the generation of a "Schrödinger cat" state of motion [38] and the tomographic measurement of nonclassical states of motion [39].

To complete this section, we give an example of how a "maximally-entangled" state of N ions might be prepared with the use of the quantum logic gates described in this section [9]. We desire to create the state

$$\Phi_{\mathrm{ME}} = \frac{|\downarrow\rangle_1\,|\downarrow\rangle_2\,|\downarrow\rangle_3 \cdots |\downarrow\rangle_N + e^{i\varphi}\,|\uparrow\rangle_1\,|\uparrow\rangle_2\,|\uparrow\rangle_3 \cdots |\uparrow\rangle_N}{\sqrt{2}} \tag{12}$$

(or equivalently, a coherent superposition of the numbers 0 and $2^N - 1$ in binary where we make the identification $|\downarrow\rangle \equiv 0$ and $|\uparrow\rangle \equiv 1$). Starting in an initial state Φ_{init} where all spins are in the $|\downarrow\rangle$ state, it is easy to show that one way to prepare Eq. (12) is to operate the following N gates on the initial state:

$$\Phi_{\mathrm{ME}} = [CN_{1,N}]\,[CN_{1,N-1}]\,[CN_{1,N-2}] \cdots [CN_{1,2}]\,[R_1(\pi/2,\,\varphi)]\,\Phi_{\mathrm{init}}\,, \tag{13}$$

where $CN_{i,j}$ denotes the controlled-NOT operator with ion i as the control bit and ion j as the target bit, and the rotation operator is applied to the first ion. The state Φ_{ME} can be viewed as the N-particle generalization of the entangled pair states envisioned by EINSTEIN, PODOLSKY, and ROSEN [40], and may find uses in improved atomic spectroscopy and frequency standards [7, 8].

IV. Packing Ions into a Trap

The reduced CN gate demonstrated in [10] involved only a single ion, and is therefore not useful for computation. Future experimental work will concentrate on scaling the system up by packing more ions into the trap and improving the gate fidelity, thereby allowing more gates to be coherently performed. In this section, we survey selected experimental problems which may arise in the scaleup. For a more extensive coverage of the scaling problem, see Ref. [11].

A. Individual ion addressing

One major concern in extending quantum logic to larger numbers of ions is the requirement that ions be individually addressed with laser beams for logic operations. This may be difficult, because the high vibrational frequencies desired for efficient laser cooling and suppression of decoherence also results in closely spaced ions. It can be shown that the minimum separation of adjacent ions in a linear trap between the center ions scales approximately as $s_{\min} \simeq 2sN^{-0.56}$, with $s = (q^2/4\pi\varepsilon_0 m\omega_z^2)^{1/3}$, where N is the number of ions [12, 13]. For $^9Be^+$ ions with an axial COM frequency of $\omega_z/2\pi = 1$ MHz, this separation is about 10 μm for 2 ions, and 4 μm for 10 ions.

The most straightforward method for individual optical addressing is to tightly focus laser beams on the selected ion [9]. The transverse intensity distribution of a Gaussian optical beam of power P is

$$I(r) = \frac{2P}{\pi w_0^2}\exp\left(-\frac{2r^2}{w_0^2}\right), \tag{14}$$

where $w_0 \simeq \lambda(\pi \cdot NA)$ is the beam waist, λ the radiation wavelength, and $NA = \tan\theta$ is the numerical aperture of the beam with cone half-angle θ (the formula for w_0 in the paraxial ray approximation is valid only for $NA < 1$) [41]. For large numerical apertures ($NA \approx 0.5$), it appears that laser beams can thus be focussed down to a spot on the order of a wavelength, but this is difficult to realize in the laboratory. If we can realize $w_0 = 5\,\mu\text{m}$ in a Gaussian beam, then at a distance 10 μm from the center of the beam this would imply a relative intensity of about $3 \cdot 10^{-4}$ or a electric field amplitude (proportional to Rabi frequency) of 1.8% relative to the center of the beam. If $w_0 = 2\,\mu\text{m}$ could be obtained, the intensity (electric field) would be down by a factor of $1.3 \cdot 10^{-14}$ ($1.1 \cdot 10^{-7}$). These results are likely too optimistic, since imperfections in the surfaces of the intervening vacuum port window, multiple reflections from these windows, and diffraction will typically distribute laser intensity outside of the theoretical waist of the beam. The degree to which this occurs depends on the details of window surfaces, etc. and must be resolved experimentally.

Tightly focussed Gaussian beams possess high transverse intensity gradients, resulting in the potential for significant intensity fluctuations at the selected ion if the relative position of the beam with respect to the ion is not stable on the time scale of the computation. An alternative to using tightly focussed Gaussian laser beams is to first feed the (expanded) laser beam through a sharply defined aperture (slit or aperture), and use a lens to image the aperture at the position of the ions. With this technique, the beam intensity can be distributed more smoothly around the selected ion and have very steep intensity edges (on the order of the original aperture sharpness) away from the ion, thus suppressing beam vibration problems and confining the radiation to a single ion. This technique has been used to make relatively "hard" walls for an optical dipole trap [42]. For this technique to work well, the imaging lens must collect a large fraction of the light transmitted through the aperture or else diffraction effects will result in light intensity outside the image of the aperture. To address individual ions, we require very small aperture images, which gives rise to a design tradeoff. If a one-to-one relay lens is used to image a small object aperture, effects of diffraction are enhanced. If a demagnifying lens is used to reduce a large object aperture, then the aperture must be placed a large distance from the lens, requiring a relatively large lens. For two ions, imaging a sharp edge such as a razor blade at the space between the ions may be sufficient. We might also consider having every other ion in a string be a "garbage" ion which is not used in the computation, thereby increasing the spacing between qubit ions by a factor of two (or more, if more garbage ions are used between each qubit ion). This has the disadvantage that total number of ions (and spectator modes) increases, aggravating the problems associated with large quantum registers. If sufficiently good addressing on one ion in a string can be accomplished, it may be simpler to shift the ions, rather than the laser beams, in order to address different ions. This could be accomplished by applying different static potentials U_0 and U_0' to the end segments of the rods in Fig. 2. However, changes in U_0 and U_0' would have to be coordinated to keep the COM axial frequency constant or else additional phase shifts would be introduced. Stimulated-Raman transitions have the advantage that the effective wavevector $\delta\boldsymbol{k} = \boldsymbol{k}_1 - \boldsymbol{k}_2$ can be made parallel to the axis of the trap even though each beam is at an angle with respect to the trap axis. This would allow selection of a particular ion, while eliminating coupling to transverse modes.

Another method of optically addressing individual ions is to cause a destructive optical interference at the position of a specific ion, with a net coupling at the other ion(s). For instance, if ion j is positioned at the node of a resonant standing wave laser field, the coupling between states $|n\rangle\,|\downarrow\rangle_j$ and $|n'\rangle\,|\uparrow\rangle_j$ is proportional to $\langle n'|\sin[\eta_j(a + a^\dagger)]\,|n\rangle$. In this case, the coupling of the standing wave to ion j vanishes when the laser frequency is tuned to an even order sideband such as the carrier ($n' = n$). If, instead, the ion is positioned at an antinode, the coupling is proportional to $\langle n'|\cos[\eta_j(a + a^\dagger)]\,|n\rangle$; thus, the coupling

vanishes when the laser frequency is tuned to an odd order sideband, such as the first blue or red sideband ($n' = n \pm 1$). By choosing the angles of focussed laser beams relative to the trap axis appropriately, it should be possible to position an antinode (node) at ion j while approximately positioning nodes (antinodes) at the ions adjacent to ion j (for equally spaced ions). In the case of two-photon stimulated Raman transitions, we desire to place ion j at a common node or antinode of two standing waves. Although this interference technique should allow individual access to each of two trapped ions, it appears technically difficult to extend this technique to more than three ions.

Next, we consider the application of external field gradients which shift the internal energy levels of ions depending on their position. For a magnetic field gradient to give this selectivity, we require the Zeeman splitting between adjacent ions to be much larger than the Rabi frequency, or $\Delta\mu(\partial|\boldsymbol{B}|/\partial z)\, s/\hbar \gg \Omega$, where $\Delta\mu$ is the difference in $\langle\mu \cdot \boldsymbol{B}\rangle/|\boldsymbol{B}|$ between the two levels of interest, and s is the ion separation along the z direction. For $\Delta\mu = \mu_B$, $s = 10\,\mu\text{m}$, and a Rabi frequency of $\Omega/2\pi \approx 1\,\text{MHz}$, this requires $\partial|\boldsymbol{B}|/\partial z \gg 0.1\,\text{T/cm}$. Field gradients of this magnitude can be achieved; however, they might introduce large and uncontrollable phase shifts for the other ions in a quantum register.

The laser beam itself can provide ion selectivity by employing the transverse gradient in the optical field intensity. For instance, if we desire to perform a θ-pulse on ion j without affecting neighboring ion k, the intensity profile of the laser beam can be set so that the ratio of field strengths (intensities for the case of two-photon stimulated-Raman transitions) at ion j vs. ion k is $\theta/2\pi m$, where m is an integer. Now if the pulse duration is set so that ion j is rotated by θ, ion k receives a rotation of $2\pi m$ and hence returns back to its initial state (with an extra phase factor of $(-1)^m$).

For the case of two-photon stimulated-Raman transitions, the laser beam can provide ion frequency selectivity by employing the Stark shift and the transverse gradient of the optical field. Here, for example, we could assume that the two counterpropagating Raman beams of equal intensities and spatial profiles are offset so that beam 1 is centered on ion j, and beam 2 is centered on adjacent ion k as depicted in Fig. 5. Let ε be the fraction of peak intensity seen by the offset ions (that is, the intensity of beam 2 at ion j and beam 1 at ion k). Assume that when either beam is centered on either ion, the single photon resonant Rabi frequencies are equivalent: $g_1 = g_2 = g$. When the beams are offset, the two-photon Rabi frequency at each ion is $\Omega = \varepsilon^{1/2}(g^2/\Delta_R)$, where g^2/Δ_R is the Rabi frequency expected if both beams were centered on a given ion. The Stark shifts of the two ions are in opposite directions: $\delta_j = +\delta_0$, $\delta_k = -\delta_0$, where $\delta_0 = \Omega(1-\varepsilon)/\varepsilon^{1/2}$. If we make $\delta_0 \gg \Omega$ ($\varepsilon \ll 1$), then by appropriately tuning the difference frequency of the laser beams, we can selectively drive transitions on either ion j or k. Alternatively, if we desire to perform a θ-pulse to ion j without affecting ion k in an "unrepairable" way, ε can be tuned to a particular value which results in ion k returning to within a phase factor to its initial state. For square pulses in time, we require $\theta/2(1+\delta^2/\Omega^2)^{1/2} = m\pi$, or $\varepsilon^2 - [1 + (2m\pi/\theta)^2]\,\varepsilon + 1 = 0$, where m is an integer. For $m = 1$ and $\theta = \pi$ (a π-pulse on ion j), this occurs for $\varepsilon = 0.208$. Generalizing this to more than two ions becomes difficult if the laser beams also overlap other qubit ions. This scheme places an additional premium on laser power stability, since the light shifts are bigger than the Rabi frequencies by $1/\varepsilon^{1/2}$ for $\varepsilon \ll 1$. In addition, in both of the above schemes, employing the laser beams to differentially affect neighboring ions, one major drawback is that the positions and profiles of the laser beams must be accurately controlled.

Finally, we consider a method of addressing which utilizes rf micromotion. In a conventional Paul trap, generalized to the case of asymmetric electrodes ($\Phi \propto V_0 \cos(\Omega_T t) \times(\varepsilon x^2 + (1-\varepsilon)\, y^2 - z^2)$, $0 < \varepsilon < 1$) [43], the rf fields vanish only at a single point in space. When multiple ions are crystalized in such a trap, each ion experiences a different rf field, leading to different amounts of micromotion. In general, this effect causes each ion to have a unique Rabi frequency when a laser is applied, allowing the possibility of differen-

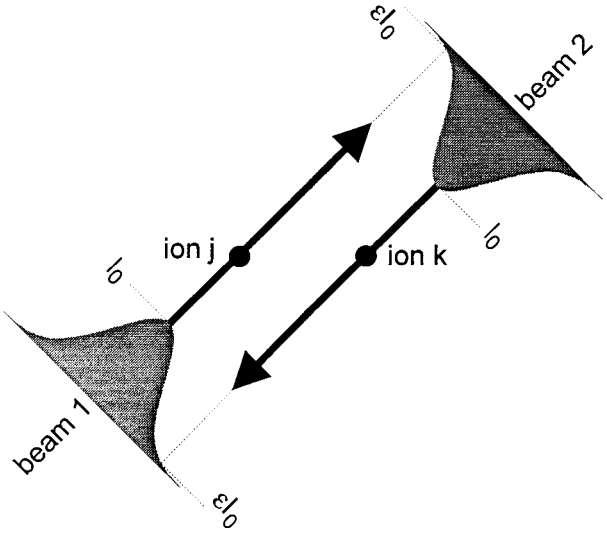

Fig. 5: Differential AC Stark shifting of neighboring ions. Equal intensity counter propagating beams 1 and 2 are centered on ions j and k, respectively. A fraction ε of the peak intensity I_0 of each beam is applied to the other ion. This results in a differential AC Stark shift of ions j and k, allowing the possibility of individually accessing the ions by tuning the frequency of the laser beams.

tial addressing of the ions. If we assume that each ion sees the same intensity laser field, the Rabi frequency of ion j is proportional to $J_0(\boldsymbol{k}\cdot\zeta_j)$ [11, 44], where $J_0(X)$ is the zeroth Bessel function of argument X, $\boldsymbol{k}$ is the effective laser wavevector, and ζ_j is the amplitude of micromotion associated with the jth ion. We assume that ion j experiences a static electric field $\boldsymbol{E}_{sj}$ (due to the Coulomb field of the other ions in addition to background static fields) which prevents the ion from occupying the trap center defined by the rf fields. For simplicity, we assume that $\boldsymbol{E}_{sj} = E_{sj}\hat{\boldsymbol{x}}$ is along the x axis of the trap, which should be the case if the ions crystalize along the x-axis ($\varepsilon < 0.5$). To estimate ζ_j, we solve the classical equations of motion in the trap for $U_0 = 0$ and find $= \zeta_j\cdot\hat{\boldsymbol{x}} = \sqrt{2}\,qE_{sj}/m\omega_x\Omega_T$, where ω_x is the x-axis COM secular harmonic frequency. Thus, the Rabi frequency of the jth ion is

$$\Omega^j = \Omega_0^j J_0\left(\frac{\sqrt{2}\,k_x q E_j}{m\omega_x\Omega_T}\right), \tag{15}$$

where Ω_0^j is the Rabi frequency in absence of micromotion. (This reduction of the Rabi frequency due to ion motion is treated in section IV.B.1. under a different context.) Thus by controlling the electric field E_j at the jth ion, some degree of differential addressing of the ions is possible. For example, for three ions held along the x-axis with the middle ion placed exactly at the rf null position, we find that the ratio of Rabi frequencies of the outer ions to the middle ion is $J_0(\beta)$, where $\beta = 1.52k_x(q^2\omega_x/4\pi\varepsilon_0 m)^{1/3}/\Omega_T$. An interesting case for individual addressing occurs when $\beta = 2.405$, in which case $J_0(\beta) = 0$, and the laser interaction with the outer two ions is effectively shut off. For three $^9Be^+$ ions held in a trap with a rf drive frequency of $\Omega_T \approx 240$ MHz, we find that the Rabi frequency of the outer two ions vanishes at a COM secular frequency of $\omega_x/2\pi \approx 6.1$ MHz. Here we assume that the Rabi frequency describes a stimulated Raman coupling between hyperfine ground states with $k_x = \sqrt{2}\,(2\pi/\lambda)$ and $\lambda \approx 313$ nm, relevant to recent experiments [10].

Many of the above individual addressing schemes are improved greatly when dealing with only two ions instead of a string of many. This leads us to seriously consider systems where quantum logic operations are performed on accumulators consisting of only two ions, with the other ions located somewhere else. For example, pairs of ions may be held in different regions of the same trap structure [11], or quantum information may be transferred from one register of ions to another by optical means [45].

B. Multimode interference

Each additional ion in a quantum register adds three more motional modes. The simplest form of the Cirac/Zoller scheme ideally uses just a single mode as the bus. In this section, a few potential problems associated with the $3N-1$ spectator modes are considered. First, we must generalize the interaction with electromagnetic fields discussed in section II.B to consider motion in all $3N$ modes of motion for N trapped ions. Here, as was assumed by CIRAC and ZOLLER [9], we consider that, on any given operation, the laser beam(s) interacts with only the jth ion; however, that ion will, in general, have components of motion from all modes. In this case Eq. (3) for the jth ion becomes

$$H_I^j = \hbar\Omega^j(S_+^j + S_-^j)\,[e^{i(\boldsymbol{k}\cdot\boldsymbol{x}_j-\omega t+\varphi_j)} + \text{h.c.}]\,. \tag{16}$$

We write the position operator of the jth ion (which represents the deviation from its equilibrium position) as

$$\boldsymbol{x}_j = \boldsymbol{u}_j\hat{\boldsymbol{x}} + \boldsymbol{u}_{N+j}\hat{\boldsymbol{y}} + \boldsymbol{u}_{2N+j}\hat{\boldsymbol{z}}\,, \quad j\in\{1,2,,\ldots N\}\,, \tag{17}$$

where the u_p are related to the $3N$ normal mode coordinates q_k $(k\in\{1,2,\ldots 3N\}$ by the following relations [46]

$$\boldsymbol{u}_p = \sum_{k=1}^{3L} D_k^p q_k\,, \qquad q_k = \sum_{p=1}^{3L} D_k^p \boldsymbol{u}_p\,, \quad q_k \equiv q_{k0}(a_k\,e^{-i\omega_k t} + a_k^\dagger\,e^{i\omega_k t})\,. \tag{18}$$

In this expression, q_k is the position operator and a_k and $a_k^\dagger$ are the associated lowering and raising operators for for the kth normal mode, and the matrix D_k^p is the transformation matrix between physical coordinates of the individual ions and normal coordinates of the string. Following the procedure of section II.C, we find

$$H_I^j = \hbar\Omega^j\left(S_+^j \exp\left[i\sum_{k=1}^{3L}\eta_k^j(a_k\,e^{-i\omega_k t} + a_k^\dagger\,e^{i\omega_k t}) - i(\delta t-\varphi_j)\right] + \text{h.c.}\right), \tag{19}$$

where we have kept the time dependence to allow consideration of all motional modes with different frequencies, and $\delta=\omega_L-\omega_0$ is the detuning of the applied radiation frequency (or difference frequency for the Raman coupling). The generalized Lamb-Dicke parameters are $\eta_k^j \equiv (\boldsymbol{k}\cdot\hat{\boldsymbol{x}}D_k^j + \boldsymbol{k}\cdot\hat{\boldsymbol{y}}D_k^{N+j} + \boldsymbol{k}\cdot\hat{\boldsymbol{z}}D_k^{2N+j})\,q_{k0}$, but for the linear trap case, motion will be separable in the x, y, and z directions and η_k^j will consist of one of these terms. We are typically interested in coupling the internal states of a given ion j to a selected mode of collective motion k. In this case, the Rabi frequency coupling the states $|n_k\rangle\,|\downarrow\rangle_j$ to $|n_k'\rangle\,|\uparrow\rangle_j$ is

$$\Omega_{n_k',n_k}^j \equiv \Omega^j\,|\langle\{n_{p\neq k}\},\,n_k'|\prod_{l=1}^{3N} e^{i\eta_l^j(a_l+a_l^\dagger)}\,|\{n_{p\neq k}\},\,n_k\rangle|\,. \tag{20}$$

where $|\{n_{p\neq k}\}\rangle$ denotes the state of motion of the $3N-1$ spectator modes excluding mode k.

1. Effects of motion in spectator modes on logic gates (Debye-Waller factors)

From the last equation, the Rabi frequency of a particular operation will in general depend on the motional state of the spectator modes. For instance, the conventional controlled-not gate employs two carrier pulses (steps (a) and (c) in Sec. III) which ideally do not depend

on the state of motion; this requires the Lamb-Dicke parameter η to be small (see Eq. (10)). In the Raman configuration, η is proportional to the difference in two wavevectors and can be made negligible by using co-propagating beams ($\delta\boldsymbol{k} \approx 0$). On the other hand, with single-photon optical transitions, the Rabi frequencies depend on the motion of all modes which have a component of motion along the direction of $\boldsymbol{k}$. We can take advantage of the motional dependence of the carrier to construct a logic gate, but in this case also, the Rabi frequency will depend on the motion in the other modes along the direction of $\boldsymbol{k}$ or $\delta\boldsymbol{k}$. Similarly, for sideband operations, such as steps (1) and (3) of the CN scheme discussed in Sec. III, it will, in general, be impossible to have $\Omega^j_{n',n}$ depend on only one mode of motion. In this section, we examine the influence of extraneous modes on the Rabi frequencies $\Omega^j_{n',n}$.

In a collection of N ions, the motion in the $3N-1$ spectator modes reduces the Rabi frequency in much the same way as lattice vibrations affect a single emitter or scatterer embedded in a crystal, as described by the Debye-Waller effect [47]. Typically, the motional quantum numbers of the spectator modes in Eq. (20) will be thermally distributed (i.e., $P(n_p) \propto \gamma^{n_p}$ where $\gamma = \bar{n}_p/(1+\bar{n}_p)$ with $\bar{n}_p$ the mean number of phonons in mode p), so we can calculate the rms and mean values of the Rabi frequency given this distribution. For simplicity, we assume that all spectator modes are in the Lamb-Dicke regime ($\eta_p^j \bar{n}_p^{1/2} \ll 1$), but see Ref. [11] for the more general case. If the frequencies and amplitudes of all modes contributing to the axial motion of ion j are assumed to be about the same, we can write $\eta_p^j \simeq \eta/N^{1/2}$ and $\bar{n}_p \simeq \bar{n}$ where η and $\bar{n}$ are the Lamb-Dicke parameter and mean occupation for the axial motion of a single (thermalized) trapped ion. In this case, the fractional fluctuation in the Rabi frequency from run to run is

$$\frac{\Delta\Omega^{j,\,rms}_{n'_k,n_k}}{\bar{\Omega}^j_{n'_k,n_k}} \simeq \eta^2 \sqrt{\frac{\bar{n}(\bar{n}+1)}{N}} \,. \tag{21}$$

This expression indicates that a large number of ions is beneficial because it tends to average out the effects of motion in the $N-1$ spectator modes. Eq. (21) is an overestimate of the fluctuations since the spectator modes will have higher frequency than the COM mode, leading to smaller amplitudes of motion than assumed in this crude estimate. In any case, it is clearly desirable to cool all modes (whose motion is parallel to $\delta\boldsymbol{k}$) to the zero-point state ($\bar{n}_p = 0$) to suppress the effects of these Debye-Waller factor fluctuations.

2. Mode cross-coupling from static electric field imperfections

If the $3N-1$ spectator modes of oscillation are not all laser-cooled to their zero-point energy, then energy can be transferred to the kth mode of interest. Even when the spectator modes are cooled to the zero-point state, they can act as a reservoir for energy from the COM mode. This does not lead to heating but can cause decoherence.

Ideally, the ions are subjected to quadratic potentials as in Sec. II.B. In practice, higher-order static potential terms are present; these terms can induce a coupling between the modes. Similar couplings are induced by the time varying fields necessary for providing entanglement; these are discussed below. We will assume that the higher order field gradients act as a perturbation to the (harmonic) normal mode solution. Following the convention in the above introduction to Sec. IV.B, these fields will be specified by E_i for $i \in \{1, 2, \ldots 3N\}$ where the index i specifies both the ion and direction of $\boldsymbol{E}$. We write the electric field at the jth ion as

$$\boldsymbol{E}_j = E_j\hat{\boldsymbol{x}} + E_{N+j}\hat{\boldsymbol{y}} + E_{2N+j}\hat{\boldsymbol{z}}\,, \quad j \in \{1, 2, \ldots N\}\,. \tag{22}$$

From Eqs. (18) and (21), we can write the equation of the kth normal mode as [46]

$$\frac{\partial^2 q_k}{\partial t^2} + \omega_k^2 q_k = \frac{q}{m} \sum_{i=1}^{3N} D_k^i E_i \,. \tag{23}$$

In general, we can write

$$\begin{aligned} E_i &= E_i(\{u_p\}) = E_i(\{q_j\}) \\ &= E_i(\{q_j\} = 0) + \sum_{m=1}^{3N} q_m \left[\frac{\partial E_i}{\partial q_m}\right]_{\{q_j\}=0} + \frac{1}{2} \sum_{l=1}^{3L} \sum_{m=1}^{3N} q_l q_m \left[\frac{\partial^2 E_i}{\partial q_l \, \partial q_m}\right]_{\{q_j\}=0} + \dots \,, \end{aligned} \tag{24}$$

where the derivatives are evaluated at the equilibrium positions. The first term on the right side of the last equation just gives rise to a shift of the equilibrium positions, and the second term can be absorbed into new definitions of the normal mode frequencies ω_i. The second-order term (last term shown in this equation) can resonantly couple two modes of oscillation (l and m) to the normal mode of interest k. We find a possible resonant term:

$$\frac{\partial^2 q_k}{\partial t^2} + \omega_k^2 q_k = \frac{q}{m} \sum_{i=1}^{3N} D_k^i q_l q_m \left[\frac{\partial^2 E_i}{\partial q_l \, \partial q_m}\right]_{\{q_j\}=0} , \tag{25}$$

where the l and m mode frequencies satisfy $|\omega_l \pm \omega_m| = \omega_k$. This type of coupling can either add to or extract energy from mode k, depending on the relative phases of motion in the three modes. By substituting the free solution to modes l and m $(q_j(t) = Q_k \exp(\pm i(\omega_j t + \varphi_j))$ into the second-order term, we find that if $q_k\,(t=0) = (dq_k/dt)_{t=0} = 0$, the driven solution to the amplitude of mode k initially grows linearly with time:

$$|q_k(t)| = \left| \frac{qt}{2m\omega_k} \sum_{i=1}^{3N} D_k^i Q_l Q_m \left[\frac{\partial^2 E_i}{\partial q_l \, \partial q_m}\right]_{\{q_j\}=0} \right| . \tag{26}$$

We illustrate with an approximate numerical example which might have been expected to play a role in the motional heating that was observed in the NIST experiments [10, 17] (see section V.B below). In those experiments, performed on single $^9Be^+$ ions, the heating that was observed on the motion in the x direction was such that the ion made a transition from the $n = 0$ to $n = 1$ level in about 1 ms. For a single ion, the three normal modes are just the oscillation modes along the x, y, and z directions ($q_1 = x$, $q_2 = y$, $q_3 = z$; $D_k^i = \delta_k$). The mode frequencies were $(\omega_x, \omega_y, \omega_z)/2\pi \simeq (11.2, 18.2, 29.8)$ MHz, thus approximately satisfying the condition $\omega_x + \omega_y = \omega_z$. For sake of argument, we assume this resonance condition to be exactly satisfied. We consider heating of the x motion assuming both the y and z modes are excited. From Eq. (26), we find $|x(t)| = |qtA_yA_z[\partial^2 E_x/\partial y\,\partial z]_{(y=z=0)}/(2m\omega_x)|$ where A_y and A_z are the amplitudes of motion in the y and z directions. Here, we neglect the fact that energy is exchanged between the three modes; for simplicity we assume the amplitudes of the y and z motion remain fixed. In this approximation, if $A_y = A_z = \xi$, the time it takes to excite the x motion to the same amplitude is given by $t = |2m\omega_x/(q\xi[\partial^2 E_x/\partial y\,\partial z]_{(y=z=0)})|$. If $\xi = 10$ nm (corresponding to $\langle n_y\rangle \simeq \langle n_z\rangle \simeq 1$ for the conditions of the single $^9Be^+$ ion NIST experiments, the field gradient required to drive the x motion to an amplitude of 10 nm ($\langle n_x\rangle \simeq 1$) in the

observed time of 1 ms is approximately $\partial^2 E_x/\partial y\,\partial z = 1000\ \mathrm{V/mm^3}$. It is highly unlikely the gradient was this large for the NIST experiments, and, furthermore, the resonance condition was only approximately satisfied. Moreover, this source of heating was easily tested by varying the initial values of A_y and A_z (by varying the Doppler-cooling minimum temperature through laser detuning) and studying the heating rate of the x motion which had previously been cooled to the zero point of motion. No dependence on the initial values of A_y and A_z was found. In any case, if all modes of motion are initially cooled to the zero-point state this source of heating vanishes because the assumed coupling only provides an exchange of energy between modes. This places a premium on cooling all modes to as low an energy as possible. Finally, it appears that this single-ion example gives a worst case scenario since, for large numbers of ions, the force on the generalized coordinates (right hand side of Eq. (23)) requires a high-order field gradient to be nonzero. These gradients are highly suppressed in the typical case where ion-ion separation is much smaller than the distance between the ions and the trap electrodes.

3. Mode cross coupling induced by logic operations

In the preceding sections, we have assumed that when transitions are driven between $|n_k\rangle\,|\downarrow\rangle_j$ and $|n'_k\rangle\,|\uparrow\rangle_j$ involving a single mode of motion k, the other $3N-1$ spectator modes of motion are not affected because coupling to them is nonresonant. However, when the sum or difference frequency of two or more spectator modes is near the frequency of the desired mode-k transition ($\omega_k\,|n'_k - n_k|$), higher order couplings can entangle the $|n_k\rangle\,|\downarrow\rangle_j$ and $|n'_k\rangle\,|\uparrow\rangle_j$ states with the spectator mode states.

Equation (19) describes the general interaction Hamiltonian between the internal levels of ion j and all $3N$ modes of motion. By expanding the exponential in Eq. (19) to all orders, we find

$$H_I^j = \hbar\Omega'_j \left[S_+^j \left(\prod_{l=1}^{3N} \sum_{b_l,\,d_l=0}^{\infty} \frac{(i\eta_l^j a_l^\dagger)^{b_l}\,(i\eta_l^j a_l)^{d_l}}{b_l!\,d_l!}\; e^{i(b_l-d_l)\,\omega_l t} \right) e^{i(\delta t-\varphi_j)} + \mathrm{h.c.} \right], \qquad (27)$$

where $\Omega'_j = \Omega^j \exp\left[-\frac{1}{2}\,\Sigma_l(\eta_l^j)^2\right]$. This equation describes the processes of each mode l gaining or losing $(b_l - d_l)$ vibrational quanta, accompanied by the raising or lowering of the internal electronic levels of ion j. We must account for all terms in Eq. (27) which do not vary rapidly in time, or terms in which the resonance condition is nearly met: $\Sigma_l(b_l - d_l)\,\omega_1 \simeq \delta = \omega_k(n'_k - n_k)$. Although detailed treatment of this problem is beyond our intent, a couple of comments may be made.

In general, we must account for all the terms in Eq. (27) which cause significant errors in the overall computation we are trying to carry out. For two or more trapped ions, some combination of modes will nearly always satisfy the resonance condition. However, this may occur only for high orders of b_l and d_l, and if the Lamb-Dicke criterion is met, the contributions are vanishingly small. The terms that will cause problems are the ones that are close to satisfying the resonance condition and are relatively low order in b_l and d_l. If the Lamb-Dicke criterion is satisfied, it will always be possible to avoid these spurious couplings, but it may be at the expense of making the Rabi frequency so small (in order to avoid coupling to relatively nearby off-resonant terms) that the operations will become too slow.

To understand this problem in the context of a simple example, we assume that a cross-mode coupling of this type occurs when two modes, p and q, have frequencies which satisfy the condition $n_p\omega_p - n_q\omega_q \simeq 0$, ω_k, or $-\omega_k$ corresponding to possible extraneous mode coupling on the carrier, first blue sideband, or first red sideband of the logic operations (assumed to utilize mode k). This additional resonance condition yields, to lowest

order in the Lamb-Dicke parameters, the effective Hamiltonian

$$H_I^j = \hbar\Omega_j' S_+^j \left\{ 1 + i\eta_k^j (a_k\, e^{-i\omega_k t} + a_k^\dagger\, e^{i\omega_k t}) + \frac{(i\eta_p a_p^\dagger)^{n_p}\,(i\eta_q a_q)^{n_q}}{n_p! n_q!}\, e^{i(n_p\omega_p - n_q\omega_q)\,t} \right\} e^{-i(\delta t - \varphi_j)} + \text{h.c.}\,, \tag{28}$$

where the resonance conditions are given by $\delta \equiv \omega_L - \omega_0 = 0$, $+\omega_k$, or $-\omega_k$. A specific example is relevant to the NIST single $^9Be^+$ ion experiments. Here, mode k was the x oscillation, and modes p and q are identified with the z and y oscillations of the single ion in the trap. In this experiment $\eta_x = \delta\boldsymbol{k}\cdot\hat{\boldsymbol{x}}x_0$, $\eta_y = \delta\boldsymbol{k}\cdot\hat{\boldsymbol{y}}y_0$, $\eta_z = \delta\boldsymbol{k}\cdot\hat{\boldsymbol{z}}z_0$, and $\omega_x \simeq \omega_z - \omega_y$. (The frequency relationship $\omega_x = \omega_z - \omega_y$ is a consequence of Maxwell's equations for a quadrupole rf trap in the absence of static potentials applied to the electrodes [43]) We assume that the desired transition is the first blue sideband of mode $x\,(\delta = \omega_x)$. In this case, the resonant part of Eq. (28) becomes

$$H_I^j = \hbar\Omega_j'[S_+^j\{i\eta_x a_x^\dagger - \eta_z\eta_y a_z^\dagger a_y + O(\eta^3)\} + \text{h.c.}]\,. \tag{29}$$

The term proportional to $a_x^\dagger$ is the desired anti-Jaynes-Cummings operator, and the term proportional to $a_z^\dagger a_y$ can entangle the internal state with the other spectator modes (z and y), leading to errors.

For logic operations on a string of ions in a linear trap, we will assume that all other mode frequencies are higher. With the use of stimulated-Raman transitions, we can make $\delta\boldsymbol{k} \parallel \hat{\boldsymbol{z}}$ and restrict our attention to spectator modes along the z axis. Nevertheless, as N becomes large, nearby resonances of the type shown in Eq. (28) will become harder to avoid. These coupling terms always scale as products of Lamb-Dicke parameters. Thus if the spectator mode Lamb-Dicke parameters are small enough, or if at least one Lamb-Dicke parameter is approximately zero, the higher order unwanted resonances may be sufficiently suppressed. Furthermore, if the spectator modes are cooled to near the zero-point energy ($\langle n\rangle \ll 1$), then any couplings in Eq. (28) with powers of the annihilation operator a_q will be absent most of the time. Hence, in large registers, it will probably be important to cool all modes to near the zero-point energy.

V. Decoherence

A. Internal state decoherence from spontaneous emission

The internal atomic states of trapped ions, which store quantum bits of information, must be protected from spontaneous emission, at least for the duration of the computation. This excludes the possibility of "error correction," [48] which can tolerate a certain level of errors due to spontaneous emission. For qubit levels coupled by single photon optical transitions, this may be accomplished by employing long-lived energy levels which do not have an allowed electric dipole coupling, such as metastable electronic levels with a quadrupole or intercombination coupling to the ground state. Although the interaction of these states with the vacuum (causing spontaneous emission) is reduced, their interaction with an external field for use in quantum logic operations is also reduced. This results in a fundamental limit on the accuracy of each operation by roughly the ratio of the spontaneous emission rate to the Rabi frequency $\xi = \Gamma/\Omega$. In the case of optical transitions, Ω cannot be increased indefinitely, since at optical intensities beyond about 10^{14} W/cm^2, the atom is quickly photoionized. This amounts to inaccuracies due to spontaneous emission on the order of $\xi = 10^{-6} - 10^{-7}$ [49]. Even this limit may be too optimistic, as the two-level

approximation breaks down before photoionization occurs, and the coupling to other electronic levels must also be considered [49]. This results in inaccuracies due to spontaneous emission on the order of $\xi = 10^{-5} - 10^{-6}$, depending on the particular ion used.

In the case of two-photon stimulated-Raman transitions between stable electronic ground states, the ratio of spontaneous emission rate to Rabi frequency is approximately $\xi_{SR} = \gamma_{se}/(g^2/\Delta)$, where $\gamma_{se} \approx \Gamma g^2/\Delta^2$ is the off-resonant spontaneous emission rate, g is the resonant single-photon Rabi frequency of each laser beam, and Δ is the detuning of the Raman beams from the excited state. This results in an inaccuracy Γ/Δ due to spontaneous emission, which is independent of optical intensity. Since Raman transitions between S electronic ground states are effective only when the detuning Δ is not much greater than the fine structure splitting of the atom [50]; this results in an inaccuracy ξ_{SR} due to spontaneous emission in range from about 10^{-4} ($^9Be^+$) to 10^{-7} ($^{199}Hg^+$), depending on the particular ion used. Spontaneous emission from spectator electronic levels should not significantly affect this limit, provided that their splitting from the virtual excited state significantly exceeds Δ and that the single photon resonant Rabi frequencies coupling the ground states to the spectator levels are not much bigger than g [49]. These appear to be reasonable assumptions for most candidate ions.

The decohering effects of spontaneous emission can be overcome by error correction schemes. Error correction is complicated by the fact that when spontaneous emission occurs, the atoms may decay to states outside the original set of computational basis states. However, this situation can, in principle, be detected by optically pumping the ions back to the computational basis and applying the error correction schemes [49, 51].

Spontaneous emission decoherence could, in principle, be nearly eliminated by driving single-photon transitions between ground-state-hyperfine or Zeeman levels with rf or microwave radiation since spontaneous emission from these levels is negligible. This may be accomplished by coupling the internal and motional states with inhomogeneous magnetic fields [52]. The speed of sideband operations is limited by the size of the field inhomogeneity one can obtain. For example, consider an ion moving along the z-axis with a magnetic field gradient $\partial B_x/\partial z$ applied on top of a uniform magnetic field B_z along the direction of motion. In the ion's reference frame, there is an rf magnetic field which can induce transitions between the internal states. The interaction Hamiltonian is then

$$\mathcal{H} = -\boldsymbol{\mu} \cdot \boldsymbol{B} = -\mu B_z S_z - \frac{\mu(\partial B_x/\partial z)\, z_0}{4} \, (S_+ + S_-)\,(a^\dagger + a)\,, \tag{30}$$

where $\mu \approx \mu_B$ is the magnitude of the ion magnetic moment, typically near one Bohr magneton, z_0 is the spatial spread of the zero-point ion wavepacket, $S_\pm$ are the spin raising and lowering operators from Sec. II.C and a and $a^\dagger$ are the usual motional raising and lowering operators. The coupling (last term in Eq. (30)) is analogous to Eq. (3), allowing the construction of logic gates as described above. Unfortunately, this method requires very high magnetic field gradients $\partial B_x/\partial z$. For instance, in order to realize an effective Rabi frequency of 0.1 MHz ($\Omega_{\text{eff}} \approx \mu_B(\partial B_x/\partial z)\, z_0/4$), a magnetic field gradient of around 10 T/cm would be necessary, where we have assumed that the motional frequency is 1 MHz. Although these gradients aren't unreasonable in the laboratory, the residual fields that accompany the gradient will dramatically shift the internal electronic levels of the trapped ions. Moreover, it would be difficult to address selected ions because of the long wavelength of the radiation relative to typical ion spacings.

B. Motional decoherence

Although the internal states of ions may be well isolated from environmental influences, the motional states of a collection of trapped ions are expected to be more susceptible to deco-

herence. The Cirac/Zoller scheme for quantum logic [9] transfers quantum information transiently through the motional states, so any decoherence of the motion will compromise operation of any multi bit quantum gate and must be minimized. In the NIST experiments with a single ion, the motional state of all three modes was observed to absorb energy from the environment at the rate of about 1 phonon (energy $\hbar\omega_z$, where $\omega_z/2\pi \approx 10$ MHz) per millisecond from the ground state [10, 17]. Although this as of yet unexplained heating rate is not believed to be fundamental, it is of considerable interest to characterize the possible sources. There are several potential mechanisms for motional decoherence; for instance "rf heating" from rf fields in the trap [53], collisions with background atoms, fluctuating patch and contact potentials on the trap electrodes, electron field emission from the electrodes, and Ohmic loss of induced image currents in the trap electrodes [54, 55]. These and other effects, considered in Ref. [11], are not expected to be major obstacles to motional coherence in a linear ion trap.

By virtue of the electric charge of trapped ions, it is natural to consider the coupling of spurious electric fields to the motion of the ion string. In this section we relate the size of electric field noise to the expected transition rate from the quantum ground state of motion in the ion trap. Such noisy electric fields might be generated from unstable trap parameters, external radiation, thermal (Johnson) noise from resistive losses in the trap electrodes, or patch potentials from nearby surfaces.

We first consider the axial COM harmonic motion of a string of N ions at frequency ω_z. An external uniform electric field will shift the position of the trap center; an external electric field gradient will change the effective spring constant of the trap. Following the approach of SAVARD, O'HARA and THOMAS [56], who considered heating mechanisms in the context of neutral atom dipole traps, we can similarly calculate the rate Γ_0 at which the ground state of ion motion is vacated due to noisy electric fields. We find

$$\Gamma_0^{\text{axial}} = \frac{Nq^2}{4m\hbar\omega_z}\left[S_E(\omega_z) + \frac{\hbar}{4Nm\omega_z} S_{E'}(2\omega_z)\right], \tag{31}$$

where $S_E(\omega)$ is the electric field noise spectral density in $(\text{V/cm})^2/\text{Hz}$ and $S_{E'}(\omega)$ is the electric field gradient noise spectral density in $(\text{V/cm}^2)^2/\text{Hz}$. The noise densities are defined so that the mean-squared electric field and field gradient are $(2\pi)^{-1}\int_0^\infty d\omega\, S_E(\omega)$ and $(2\pi)^{-1}\int_0^\infty d\omega\, S_{E'}(\omega)$, respectively [56].

Note that contributions of electric field noise to motional heating is concentrated near resonance (ω_z) in Eq. (31), as expected for a resonantly driven harmonic oscillator. Contributions of electric field gradient noise to heating is concentrated near twice the resonant frequency $(2\omega_z)$, as expected for a parametrically driven harmonic oscillator. For modes of motion with secular frequency ω_x derived from ponderomotive rf forces (i.e., the radial modes of a linear trap), there are additional contributions to heating from noisy fields at frequencies $\Omega_T \pm \omega_x$ and gradients at frequencies $\Omega_T \pm 2\omega_x$, to lowest order in the pseudopotential approximation $[(\omega_x/\Omega_T) \ll 1]$ [21]. We find

$$\Gamma_0^{\text{radial}} = \frac{Nq^2}{4m\hbar\omega_x}\left[S_E(\omega_x) + \frac{\omega_x^2}{2\Omega_T^2} S_E(\Omega_T \pm \omega_x) + \frac{\hbar}{4Nm\omega_x}\left(S_{E'}(2\omega_x) + \frac{2\omega_x^2}{\Omega_T^2} S_{E'}(\Omega_T \pm 2\omega_x)\right)\right]. \tag{32}$$

Given a source of electric field noise $S_E(\omega)^{1/2}$, we may expect the corresponding gradient noise spectrum $S_{E'}(\omega)^{1/2}$ to be no larger than $S_E(\omega)^{1/2}/d$, where d is the characteristic ion trap electrode size. From the above equations, we find that this implies that the heating rate from gradient noise is expected to be a factor of $\approx (z_0/2d)^2$ smaller than the heating

rate from electric field noise, where we recall that $z_0 = (\hbar/2Nm\omega_z)^{1/2}$ is the size of the ground state wavepacket of the mode of interest. This ratio is typically very small in ion traps (in the NIST $^9Be^+$ experiments, $z_0 \approx 7$ nm, $d \approx 250\,\mu$m, and $(z_0/2d)^2 \approx 2 \times 10^{-10}$). Noise in the electric field gradient is therefore expected to be much less of a concern than noise in the electric field, unless the electric potentials on the trap electrodes possess an unusually high degree of symmetry. It also follows that the COM modes should be most susceptible to heating, as the non-COM modes do not respond to uniform electric fields. For instance, in the case of two ions confined along the z axis, the COM mode along z is sensitive to resonant uniform electric fields. The "stretch" mode along z (where the two ions' motions are out of phase) on the other hand, is only sensitive to resonant electric field gradients. Therefore, if quantum logic operations are limited by motional heating due to uniform electric fields, higher-order (non-COM) motional modes should be used for quantum logic. COM heating will still indirectly affect the fidelity of operations on other modes, but this effect should be of higher order, as discussed in section IV.B.1.

We examine two expected sources of electric field noise, and estimate their effects on the heating rate of COM modes. These results are compared to the NIST experiment on a single $^9Be^+$ ion [17], where we observed a heating rate $\Gamma_0 \approx 10^3$/sec, corresponding to an electric field noise of $S_E(\omega_x)^{1/2} \approx 4 \cdot 10^{-8}$ V/cm/Hz$^{1/2}$ or electric field gradient noise of $S_{E'}(2\omega_x)^{1/2} \approx 0.07$ V/cm^2/Hz$^{1/2}$.

1. Thermal or blackbody noise

Thermal fluctuations from lossy elements of the trap electrode structure may lead to electric field noise at the ions. This is essentially the effect of blackbody radiation on the ion motion, altered by the "cavity" formed from the trap electrodes [11, 54, 57]. Lossy or resistive elements of the trap electrodes will only give rise to a noisy electric field only if the effective resistive current path is asymmetrically oriented with respect to the ions; otherwise only negligible field gradients will contribute, as discussed above. The voltage noise spectral density from a resistor R at temperature T is $4kTR$. For an electrode structure of characteristic size d, we thus expect an electric field noise density of $S_E(\omega) \approx 4kTR(\omega)/d^2$, where $R(\omega)$ describes the resistance seen by the ion from the surrounding electrode structure, or, equivalently, the resistance through which currents induced by ion motion flow. Neglecting the gradient terms in Eqs. (31) and (32), this results in axial and radial mode heating rates of [7, 11]

$$\Gamma_0^{\text{axial}} \approx \frac{Nq^2kTR(\omega_z)}{md^2\hbar\omega_z} \tag{33}$$

and

$$\Gamma_0^{\text{radial}} = \frac{Nq^2kT}{m\hbar\omega_x d^2}\left(R(\omega_x) + \frac{\omega_x^2}{2\Omega_T^2}\,R(\Omega_T \pm \omega_x)\right). \tag{34}$$

We now use this last equation to estimate the heating rate which might have been expected in the NIST single ion $^9Be^+$ experiments [17], where all modes were confined from ponderomotive forces. We consider two current paths in the electrode structure which would likely have provided the largest resistances. The first is a direct path between the endcap electrodes, which were positioned around the ring electrode [11, 43]. Since this path length is only about $l \approx 0.5$ cm and much smaller than the wavelengths associated with the frequencies of interest $\omega_x/2\pi \approx 10$ MHz and $(\Omega_T \pm \omega_x)/2\pi \approx 230$ MHz, we can

treat this path as a lumped resistor with resistance $R(\omega) \approx \varrho l/A(\omega)$. Here, ϱ is the resistivity of the electrode material and $A(\omega)$ is the effective cross-sectional area of the resistive path, proportional to the skin depth at frequency ω. We conservatively estimate $R(\omega_x) \approx 0.04\ \Omega$ and $R(\Omega_T \pm \omega_x) \approx 0.20\ \Omega$ in the experiment [11, 43] and calculate a heating rate of $\Gamma_0 \approx 0.7/\text{s}$, dominated by the first term of Eq. (34) and much smaller than observed.

The rf and static electrodes in an rf trap are typically joined through an rf step-up transformer. This leads us to consider a resistive path from the rf to the static electrode, as the resistance between these electrodes can be high at frequencies near the resonant rf drive frequency Ω_T. In a linear trap, these fields should not have a component along the axial modes of motion; moreover, these fields will vanish at trap center and only provide a gradient, unless there is an extreme asymmetry in the electrode structure. We thus consider noise fields resulting from a geometrical asymmetry β between the ring and endcap electrodes ($0 \le \beta \le 1$, where β is proportional to the electric field at the ion if a potential is applied between the ring and endcaps; $\beta = 0$ for perfect symmetry). In the NIST $^9Be^+$ experiments [10, 17], a quarter-wave transmision line acts as the step-up transformer [43], thus the impedance between the rf and static trap electrodes as a function of frequency ω is

$$Z_{\text{trap}}(\omega) = Z_0 \tanh\left[\frac{\pi}{4Q}\sqrt{\frac{\omega}{\Omega_T}} + i\,\frac{\pi}{2\Omega_T}\right], \tag{35}$$

where Z_0 is the characteristic line impedance, and Q is the loaded quality factor of the transmission line of length $\pi c/2\Omega_T$ at resonance ($\omega = \Omega_T$). The resistance is the real part of Eq. (35), and at the frequencies of interest which might couple to the ion motion, ω_x and $\Omega_T \pm \omega_x$, we have $R(\omega_x) \approx (\pi Z_0/4Q)\,(\omega_x/\Omega_T)^{1/2} \approx 0.03\ \Omega$ and $R(\Omega_T \pm \omega_x) \approx (Z_0/\pi Q)\,(\Omega_T/\omega_x)^2 \approx 34\ \Omega$. In these expressions, $Z_0 \approx 100\ \Omega$ and $Q \approx 500$ are the characteristic impedance and quality factor of the transformer, and $\omega_x/2\pi$ and $\Omega_T/2\pi$ are taken to be 10 MHz and 230 MHz respectively [43]. Note the estimated resistance $R(\omega_x)$ is nearly equivalent to the value in the skin-depth model above, since this path length is still only a small fraction of the wavelength associated with ω_x. We find that the two terms in Eq. (34) contribute roughly equal amounts to a total heating rate of approximately $\Gamma_0 \approx 0.8\beta^2/\text{s}$. Again, this rate is much smaller than the observed rate, even for large asymmetries.

2. Noise on trap voltages

Fluctuations in the trap voltages (U_0 and V_0 in Eq. (1)) will nominally only give rise to a noisy field gradient. However, in some cases, asymmetric fluctuations in trap parameters can give rise to a noisy electric field. For instance, noise on the static potentials of the end segments of a linear trap (Fig. 2) may not be common mode if the potentials are provided from uncorrelated power supplies, or if the leads connecting to the end segments experience different amounts of noise from pickup. In these cases, we can relate the electric field noise density to a differential potential noise density defined by $S_{\delta U_0}(\omega) = d^2 S_E(\omega)$, where δU_0 is the difference in potentials between the rod end segments. From Eq. (31), this would give rise to a heating rate of

$$\Gamma_0 = \frac{Nq^2}{4m\hbar\omega_z d^2}\, S_{\delta U_0}(\omega_z)\,. \tag{36}$$

For example, a typical power supply might have rms noise of 0.1 mV uniformly distributed across a 20 MHz bandwidth. If the supply is filtered so that signal amplitude at frequency

ω_x is attenuated by a factor $F < 1$, we find $[S_{\delta U_0}(2\omega_z)]^{1/2} \approx 20F$ (nV/Hz$^{1/2}$), leading to a heating rate of the axial COM mode of $\Gamma_0 \approx 4 \cdot 10^6 N \cdot F^2/\mathrm{s}$. Here we have assumed trap parameters $\omega_z/2\pi \approx 1$ MHz and $d \approx 0.025$ cm.

If there exist asymmetric static patch or contact potentials on the electrodes, this could lead to a static electric field $\boldsymbol{E}_{\mathrm{static}}$ which would push the ions away from at the geometrical trap center defined by $x = y = z = 0$ in Eq. (1). In this case, fluctuations in the potentials U_0 and V_0 will be converted into a noisy electric field at the ions. If $\boldsymbol{E}_{\mathrm{static}}$ is in the axial direction, then a noise density of the static voltage $S_{U_0}(\omega)$ would be equivalent to a field noise density of $S_E(\omega) = (E_{\mathrm{static}}/\langle U_0\rangle)^2 S_{U_0}(\omega)$. If we assume $E_{\mathrm{static}} \approx \varphi/d$, where φ is an effective axial potential difference across the electrodes (due to patch potentials for instance), then we find from Eq. (31)

$$\Gamma_0 = \frac{Nq^2}{4m\hbar\omega_z d^2} \left(\frac{\varphi}{\langle U_0\rangle}\right)^2 S_{U_0}(\omega_z)\,. \tag{37}$$

Similar to above, this leads to a heating rate of $\Gamma_0 \approx 4 \cdot 10^6 N \cdot F^2 (\varphi/\langle U_0\rangle)^2/\mathrm{s}$ assuming the above values of the trap parameters. Controlling these potentially troublesome heating rates clearly points to the importance of heavily filtering the static electrodes at frequency ω_z. The filtering is best accomplished as close as possible to the trap electrodes, and for reasonable filter factors of $F < 10^{-4}$, these heating sources should be negligible.

For fluctuations in the rf potential V_0, we can derive a similar heating rate of motional modes confined by ponderomotive rf forces, which would be relevant to the NIST experiments. For simplicity, we consider the COM radial mode at frequency ω_x and assume the confinement is dominated by the ponderomotive force (ω_p term in Eq. (2)). We consider the case of a patch field $E_{\mathrm{static}} = \varphi/R$. The equivalent electric field noise density is then $S_E(\omega) = (2E_{\mathrm{static}}/\langle V_0\rangle)^2 S_{V_0}(\omega)$, which from Eq. (32) results in a heating rate

$$\Gamma_0^{\mathrm{radial}} = \frac{Nq^2}{4m\hbar\omega_x R^2} \left(\frac{2\varphi}{\langle V_0\rangle}\right)^2 \left(S_{V_0}(\omega_x) + \frac{\omega_x^2}{2\Omega_T^2} S_{V_0}(\Omega_T \pm \omega_x)\right), \tag{38}$$

where $S_{V_0}(\omega)$ refers to the rf potential noise density at the trap rf electrode. To estimate the effect of rf amplitude noise at the input, we again assume that the rf input lead is connected to a step-up transformer. For a transformer of characteristic impedance Z_0 and quality factor $Q \gg \Omega_T/2\omega_x \gg 1$, input signals of frequency ω_x are essentially filtered out, and signals at $\Omega_T \pm \omega_x$ are multiplied by the factor $[Z_0/(2\pi R_s Q)]^{1/2}\, \Omega_T/\omega_x$, where R_s is the source impedance. We thus neglect the first term of Eq. (38) and replace $S_{V_0}(\Omega_T \pm \omega_x)$ by $[Z_0/(2\pi R_s Q)]\,(\Omega_T/\omega_x)^2\, S_{V_0,\,\mathrm{input}}(\Omega_T \pm \omega_x)$ in the second term. If the rf source feeding the input has an effective noise figure of $NF \approx 10$ dB above the Johnson noise of a $R_s = 50\,\Omega$ source impedance, we have $S_{V_0,\,\mathrm{input}} \approx 10(4kTR_s) \approx 10^{-17}\ \mathrm{V}^2/\mathrm{Hz}$. Assuming $\omega_x/2\pi \approx 10$ MHz, we find $\langle V_0\rangle \approx 750$ V and a heating rate of $\Gamma_0 \approx 10(\varphi/\langle V_0\rangle)^2/\mathrm{s}$. Since $\varphi \ll \langle V_0\rangle$ for typical patch potentials of < 1 V, this source of heating is again much smaller than observed. Moreover, in the NIST experiments, φ was varied over a wide range without an observed dependence on heating rate.

Although we have tried to characterize the more obvious sources of electric field noise, the actual electric field noise spectral density in an ion trap may have a complicated structure and may be difficult to characterize. The motional modes of a string of ions are most susceptible to electric field noise near the motional frequency of interest, as expected. If spurious resonances should occur at these frequencies due to background electric fields, it might be possible to avoid them by simply changing the trap param-

eters. As stated above, heavy filtering of the electrodes should provide adequate noise suppression at these frequencies and the COM motion of ions trapped in electrode structures with a high degree of symmetry will be less susceptible to electric field noise.

C. Induced decoherence from applied field amplitude noise

In the ion trap quantum computer, all operations can be traced back to Eq. (5), the coupling of states $|n\rangle|\downarrow\rangle$ to $|n'\rangle|\uparrow\rangle$. The fidelity of these operations will depend, in part, on how accurately the coupling strength Ω^j and the application time can be set. For instance, in the rotation gate of Eq. (7), the rotation angle $\theta = 2\Omega^j t$, and noise in these parameters will lead to evolution to an undesired quantum state. The effects of (Gaussian) noise on laser intensity have been treated by SCHNEIDER and MILBURN [58]. These effects show up in a well-characterized way for transitions involving Fock states. Here we briefly investigate the size of laser power fluctuations, as the Rabi frequency is proportional to the laser power in the Raman configuration. We do not examine how such errors might propagate in an extended gate structure [9, 11, 59].

Fluctuations in the laser intensity at the site of a given ion can arise from both fluctuations in the relative position of the beam with respect to the ion and fluctuations in laser power. Laser/ion position stability is particularly important since the Cirac/Zoller scheme of quantum logic assumes that ions in an array be selectively addressed, thereby requiring a high degree of control of the laser beam spatial profile (Sec. IV.A). Of course, the simplest method for minimizing position fluctuations is to employ mechanically stiff mounts for the optics and ion trap electrodes, and have the laser source as close as possible to the ions. A quadrant detector indexed to the trap electrodes and placed near the ion may also be used to actively stabilize the beam position by feeding back to a galvanometer or acousto-optic modulator. If optical fibers are used to deliver laser beams to the ions, position fluctuations between the fiber and the ions could be made small; however, we must also consider position fluctuations between the laser source and the input to the fiber. If the position tolerances can be adequately controlled, the dominant source of intensity noise at the ion would likely be given by fluctuations in optical power and laser mode. Here, we estimate limits on laser amplitude noise.

If we assume the laser fields responsible for quantum logic operations are coherent states, the fundamental noise floor is photon shot noise. For a laser beam of average power P_0 the fractional level of shot noise is

$$\frac{\delta P}{P_0} = \sqrt{\frac{\hbar\omega}{P_0\tau_{\text{op}}}}, \tag{39}$$

where ω is the (optical) photon frequency, τ_{op} is the time the radiation is applied, and, for simplicity, we assume square pulse envelopes. Almost all laser sources have significant amplitude noise well above the shot-noise limit in the 10 Hz−10 kHz range due to acoustic vibrations which, for example, affect the laser cavity resonators. Much of this noise can be removed by active power stabilization, where a beamsplitter directs a portion of the laser power to a photodetector, and an error signal is derived and fed back to an upstream modulator or, in the case of a diode laser, directly to the amplitude of the laser source [60]. The limiting noise of this stabilization scheme is degraded slightly by the imperfect quantum efficiency of the photodetector as well as the beamsplitter. If the beamsplitter directs a fraction, of the input optical power to the stabilizer (which then gives an optical power

$P_u \simeq (1-\varepsilon)P_0$ directed to the ion), and the quantum efficiency of the photo detector is η_{det}, the limit of fractional power noise in the logic pulse is (assuming no added electronic noise in the feedback loop)

$$\frac{\delta P_u}{P_u} \geq \sqrt{\frac{\hbar\omega}{P_u \tau_{\text{op}} \eta_{\text{det}} \varepsilon(1-\varepsilon)}} \,. \tag{40}$$

For a laser wavelength of 313 nm, and assuming, $\varepsilon = 0.5$, and $\eta_{\text{det}} = 0.5$, we have $\delta P_u/P_u \geq 2.3 \cdot 10^{-9}(P_\mu \tau_{\text{op}})^{-1/2}$. For 1 W of usable laser power and $\tau_{\text{op}} = 1\,\mu\text{s}$, this corresponds to a fractional power fluctuation of $\geq 2.3 \cdot 10^{-6}$.

This estimate applies only to the laser power fluctuations at the beamsplitter and assumes no additional noise is introduced between the beamsplitter and the photo detector or the beam splitter and the ions. Typically, the usable part of the laser beam must be directed further through optics, the air, and a window to the vacuum envelope enclosing the ion trap. Fluctuating etalon effects in the optics and air currents may therefore seriously increase the power fluctuations beyond Eq. (39).

Fluctuations in timing errors may also be important. Clearly, fractional fluctuations in the duration of laser pulses will correspond directly to the same fractional fluctuations in the desired value of the gate parameters (e.g., rotation angles in Eq. (7)). If we require fractional fluctuations of 10^{-6} on these parameters, then we require timing precision of 1 ps on a 1 s pulse. Similar considerations apply to the stability of pulse envelope shapes.

For both amplitude and timing fluctuations, it may be possible to sample a portion of the beam used for logic and apply it to a "check bit" ion. The response of this ion could then be used to monitor and control the amplitude and timing of the pulses.

VI. Conclusion

A system of trapped and cooled atomic ions is one of the few viable experimental candidates for quantum computation. Internal levels of the ions can coherently store quantum bits for extremely long times. Preserving coherence during logic gates will clearly be more difficult, because (1) the quantum bits are distributed through a collective motional degree of freedom in the trap which more readily couples to the environment, and (2) technical noise on the logic gates degrades gate operation. Nevertheless, to our knowledge, these difficulties appear to be technical, not fundamental. The maximum number of gates which can be applied coherently, and the maximum number of ions which can be packed into a trap, will undoubtedly be determined by technical limits. Although it appears that the quantum factoring algorithm would be extremely difficult to implement, we conclude that an ion trap quantum computer of very modest numbers of bits and gates looks quite promising.

In this paper, we have attemped to identify some of the more important experimental concerns with the ion trap system, and expect that their resolution will likely be determined in the laboratory. We summarize with a few general observations regarding the ion trap quantum computer.

(1) The most attractive coupling scheme appears to involve two-photon stimulated Raman transitions between hyperfine (or Zeeman) ground states separated by rf or microwave frequencies. This not only relaxes the laser frequency stability requirements when compared to single-photon optical transitions, but also allows more geometrical control of the effective wavevector $\delta\boldsymbol{k} = \boldsymbol{k}_1 - \boldsymbol{k}_2$, which determines the coupling to particular motional modes.

(2) Laser cooling of all modes having a component of motion along $\delta\boldsymbol{k}$ to their ground state energy will minimize cross coupling between the modes.

(3) The axial COM motional mode may not be the best choice for a "data bus" which couples the quantum bits between ions. First, although the COM mode is most resolved from the other modes, it has the lowest motional frequency, which may ultimately set a limit on the quantum gate speed. Second, the non-COM motional modes should be less sensitive to heating from external electric fields.

(4) For a given number of ions, the optimum value of the mode frequencies will likely involve a key tradeoff. Larger frequencies might minimize the effect of some sources of motional decoherence, as the motional energy levels would be further separated. This would also allow gate operations (and laser cooling) to proceed faster, as the Rabi frequency can be no larger than the mode frequency. On the other hand, smaller frequencies will increase the spatial separation of the ions, thus easing the problem of optical addressing of individual ions in a string.

(5) Internal state decoherence will likely be small, and it does not appear that motional decoherence will be a fundamental problem, notwithstanding the heating problem observed in the NIST experiments. It is important to heavily filter the ion trap static electrodes at ω_z to minimize environmental influences on the ion string COM motion.

Acknowledgements

We gratefully acknowledge the support of the U.S. National Security Agency, Army Research Office, and Office of Naval Research. We acknowledge useful discussions with P. Bardroff, R. Blatt, I. Cirac, T. Darling, L. Davidovich, A. Despain, D. DiVincenzo, A. Ekert, B. Esry, N. Gisin, S. Haroche, M. Holland, M. Holzscheiter, R. Hughes, D. James, J. Kimble, P. Knight, S. Lloyd, G. Milburn, J. Preskill, W. Schleich, A. Steane, W. Vogel, P. Zoller, and W. Zurek.

References

[1] D. P. DIVINCENZO, *Science* **270**, 255 (1995); S. LLOYD, *Scientific American* **273**, 140 (October 1995).
[2] A. EKERT and R. JOZSA, 1996, Rev. Mod. Phys. **68**, 733.
[3] D. DEUTSCH, Proc. R. Soc. London A **425**, 73 (1989); D. DEUTSCH and R. JOZSA, Proc. R. Soc. London A **439**, 554 (1992).
[4] P. SHOR, 1994, Proc. 35th Ann. Symp. Found. Comp. Sci. (IEEE Computer Society Press, New York), p. 124.
[5] S. LLOYD, *Science* **261**, 1569 (1993); **273**, 1073 (1996); L. K. GROVER, Phys. Rev. Lett. **79**, 325 (1997).
[6] *Quantum Theory and Measurement*, J. A. Wheeler and W. H. Zurek, Eds. (Princeton Univ. Press, Princeton, NJ, 1983).
[7] D. J. WINELAND, J. J. BOLLINGER, W. M. ITANO, and D. J. HEINZEN, Phys. Rev. A **50**, 67 (1994).
[8] J. J. BOLLINGER, D. J. WINELAND, W. M. ITANO, and D. J. HEINZEN, Phys. Rev. A **54**, R4649 (1996).
[9] J. I. CIRAC and P. ZOLLER, Phys. Rev. Lett. **74**, 4091 (1995).
[10] C. MONROE, D. MEEKHOF, B. KING, W. ITANO, and D. WINELAND, *Phys. Rev. Lett.* **75**, 4714 (1995).
[11] D. J. WINELAND, C. MONROE, W. M. ITANO, D. LEIBFRIED, B. E. KING, and D. M. MEEKHOF, quant-ph/9710025.
[12] A. STEANE, Appl. Phys. B **64**, 623 (1997).
[13] D. F. JAMES, Appl. Phys. B (in press), quant-ph/9702053.
[14] P. DOMOKOS, J. M. RAIMOND, M. BRUNE, and S. HAROCHE, Phys. Rev. A **52**, 3554 (1995); Q. A. TURCHETTE, C. J. HOOD, W. LANGE, H. MABUCHI, and H. J. KIMBLE, Phys. Rev. Lett. **75**, 4710 (1995); P. R. BERMAN, Ed., *Cavity Quantum Electrodynamics*, (Academic, Boston, MA, 1994).

[15] N. A. GERSHENFELD and I. L. CHUANG, Science **275**, 350 (1997); D. G. CORY, A. F. FAHMY, and T. F. HAVEL, Proc. Nat. Acad. Sci. USA **94**, 1634 (1997).
[16] J. J. BOLLINGER, D. J. HEINZEN, W. M. ITANO, S. L. GILBERT, and D. J. WINELAND, IEEE *Trans. on Instrum. and Measurement* **40**, 126 (1991).
[17] C. MONROE, D. M. MEEKHOF, B. E. KING, S. R. JEFFERTS, W. M. ITANO, D. J. WINELAND, and P. GOULD, *Phys. Rev. Lett.* **75**, 4011 (1995).
[18] W. NAGOURNEY, J. SANDBERG, and H.G. DEHMELT, Phys. Rev. Lett. **56**, 2797 (1986); TH. SAUTER, R. BLATT, W. NEUHAUSER, and P. E. TOSCHEK, Phys. Rev. Lett. **57**, 1696 (1986); J. C. BERGQUIST, R. G. HULET, W. M. ITANO, and D. J. WINELAND, Phys. Rev. Lett. **57**, 1699 (1986).
[19] M. G. RAIZEN, J. M. GILLIGAN, J. C. BERGQUIST, W. M. ITANO, and D. J. WINELAND, Phys. Rev. A**45**, 6493 (1992).
[20] W. PAUL, H. P. REINHARD, and U. VON ZAHN, Z. Phys. **152**, 143 (1958).
[21] H. G. DEHMELT, Adv. At. Mol. Phys. **3**, 53 (1967); **5**, 109 (1967).
[22] M. E. POITZSCH, J. C. BERGQUIST, W. M. ITANO, and D.J. WINELAND, Rev. Sci. Instrum. **67**, 129 (1996).
[23] B. ESRY and B. PAUL (private communication).
[24] K. E. KAHILL and R. J. GLAUBER, *Phys. Rev.* **177**, 1857 (1969); D. J. WINELAND and W. M. ITANO, *Phys. Rev.* A **20**, 1521 (1979); W. VOGEL and R. L. DE MATOS Filho, *Phys. Rev.* A **52**, 4214 (1995).
[25] D. J. WINELAND and H. G. DEHMELT, Bull. Am. Phys. Soc. **20**, 637 (1975).
[26] J. E. THOMAS, P. R. HEMMER, S. EZEKIEL, C. C. LEIBY, R. H. PICARD, and C. R. WILLIS, *Phys. Rev. Lett.* **48**, 867 (1982).
[27] M. KASEVICH and S. CHU, Phys. Rev. Lett. **69**, 1741 (1992).
[28] F. DIEDRICH, J. C. BERGQUIST, W. M. ITANO, and D. J. WINELAND, Phys. Rev. Lett. **62**, 403 (1989).
[29] D. J. WINELAND, R. E. DRULLINGER, and F. L. WALLS, Phys. Rev. Lett. **40**, 1639 (1978); W. NEUHAUSER, M. HOHENSTATT, P. TOSCHEK, and H. DEHMELT, Phys. Rev. Lett **41**, 233 (1978); D. J. WINELAND, and W. M. ITANO, *Physics Today*, vol. 40, no. 6, p. 34 (1987)
[30] B. APPASAMY, I. SIEMERS, Y. STALGIES, J. ESCHNER, R. BLATT, W. NEUHAUSER, and P. E. TOSCHEK, Appl. Phys. B **60**, 473 (1995).
[31] R. DUM, P. MARTE, T. PELLIZZARI, and P. ZOLLER, Phys. Rev. Lett. **73**, 2829 (1994); J. ESCHNER, B. APPASAMY, and P. E. TOSCHEK, Phys. Rev. Lett. **74**, 2435 (1995).
[32] G. MORIGI, J. I. CIRAC, M. LEWENSTEIN, and P. ZOLLER, Europhys. Lett. **39**, 13 (1997).
[33] D. P. DIVINCENZO, *Phys. Rev.* A **51**, 1015 (1995); A. BARENCO, *et al.*, *Phys. Rev.* A **52**, 3457 (1995); S. LLOYD, *Phys. Rev. Lett.* **75**, 346 (1995).
[34] R. P. FEYNMAN, Opt. News **11**, 11 (1985).
[35] D. M. MEEKHOF, C. MONROE, B. E. KING, W. M. ITANO, and D. J. WINELAND, *Phys. Rev. Lett.* **76**, 1796 (1996).
[36] N. F. RAMSEY, *Molecular Beams*, (Oxford University, London, 1963).
[37] C. MONROE, D. LEIBFRIED, B. E. KING, D. M. MEEKHOF, W. M. ITANO, and D. J. WINELAND, Phys. Rev. A **55**, R2489 (1997).
[38] C. MONROE, D. M. MEEKHOF, B. E. KING, and D. J. WINELAND, *Science* **272**, 1131 (1996).
[39] D. LEIBFRIED, D. M. MEEKHOF, C. MONROE, B. E. KING, W. M. ITANO, and D. J. WINELAND, Phys. Rev. Lett. **77**, 4281 (1996); J. Mod. Optics **44**, 2485 (1997).
[40] A. EINSTEIN, B. PODOLSKY, and N. ROSEN, Phys. Rev. **47**, 777 (1935).
[41] A. E. SIEGMAN, *Lasers* (University Science Books, Mill Valley, CA, 1986).
[42] S. CHU, private communication (1997).
[43] S. R. JEFFERTS, C. MONROE, E. W. BELL, and D. J. WINELAND, Phys. Rev. A **51**, 3112 (1995).
[44] D. J. WINELAND and W. M. ITANO, Phys. Rev. A **20**, 1521 (1979).
[45] J. I. CIRAC, P. ZOLLER, H. J. KIMBLE, and H. MABUCHI, Phys. Rev. Lett. **78**, 3221 (1997); S. J. VAN ENK, J. I. CIRAC, and P. ZOLLER, Phys. Rev. Lett. **78**, 429 (1997).
[46] H. GOLDSTEIN, *Classical Mechanics* (Addison-Wesley, Reading, MA, 1950).
[47] H. FRAUENFELDER, *The Mossbauer Effect*, (Benjamin, New York, 1963); H. J LIPKIN, *Quantum Mechanics* (North Holland, Amsterdam, 1973), Chaps. 2–4.
[48] P. W. SHOR, Phys. Rev. A **52**, R2493 (1995); A. STEANE, Phys. Rev. Lett. **77**, 793 (1996); Proc. R. Soc. Lond. A **452**, 2551 (1996); R. LAFLAMME, C. MIQUEL, J. P. PAZ, and W. H. ZUREK, Phys. Rev. Lett. **77**, 198 (1996); D. P. DIVINCENZO and P. W. SHOR, Phys. Rev. Lett. **77**, 3260 (1996).

[49] M. B. PLENIO and P. L. KNIGHT, Phys. Rev. A **53**, 2986 (1996); M. B. PLENIO, V. VEDRAL, and P. L. KNIGHT, Phys. Rev. A **55**, 67 (1997).
[50] R. A. CLINE, J. D. MILLER, M. R. MATTHEWS, and D. J. HEINZEN, Optics Letters, **19**, 207 (1994).
[51] J. I. CIRAC, T. PELLIZZARI, and P. ZOLLER, *Science* **273**, 1207 (1996).
[52] H. HARDE, H. LEHMITZ, J. HATTENDORF-LEDWOCH, and R. BLATT, Appl. Phys. B **53**, 131 (1991); D. J. WINELAND, J. J. BOLLINGER, W. M. ITANO, F. L. MOORE, and D. J. HEINZEN, Phys. Rev. A **46**, R6797 (1992).
[53] H. WALTHER, *Adv. At. Mol. Phys.* **31**, 137 (1993).
[54] D. J. WINELAND and H. G. DEHMELT, J. Appl. Phys. **46**, 919 (1975).
[55] J. R. ANGLIN, J. P. PAZ, and W. H. ZUREK, Phys. Rev. A **55**, 4041 (1997).
[56] T. A. SAVARD, K. M. O'HARA, and J. E. THOMAS, Phys. Rev. A **56**, R1095 (1997).
[57] A. J. DAHM and D. N. LANGENBERG, Am. J. Phys. **43**, 1004 (1975).
[58] S. SCHNEIDER and G. J. MILBURN, quant-ph/9710044.
[59] C. MIQUEL, J. P. PAZ, and W. H. ZUREK, Phys. Rev. Lett. **78**, 3971 (1997).
[60] N. C. WONG, J. L. HALL, J. Opt. Soc. Am. **B2**, 1527 (1985); C. C. HARB, M. B. GRAY, H.-A. BACHOR, R. SCHILLING, P. ROTTENGATTER, I. FREITAG, and H. WELLING, IEEE J. Quant. Elec. **30**, 2907 (1994).

(Manuscript received: September 19, 1997)